

MECHANISMS OF PLATELET CAPTURE UNDER VERY HIGH SHEAR

A Thesis
Presented to
The Academic Faculty

By

Peter J. Wellings

In Partial Fulfillment
Of the Requirements for the Degree
Master of Science in Bioengineering

Georgia Institute of Technology

May 2011

MECHANISMS OF PLATELET CAPTURE AT VERY HIGH SHEAR

David N. Ku
School of Mechanical Engineering
Georgia Institute of Technology

Cheng Zhu
School of Biomedical Engineering
Georgia Institute of Technology

Todd Sulchek
School of Mechanical Engineering
Georgia Institute of Technology

Date Approved March 30, 2011

ACKNOWLEDGEMENTS

I would like to thank Dr. David Ku for all his support throughout my graduate school experience. Thanks to Dr. Ku, I was fortunate enough to be presented many great opportunities in such a short time. I learned a great deal about managing my own projects and navigating the research environment.

I would also like to thank the current and former members of the Ku Lab who were eager to lend an ear or share a laugh. Thanks to my friends David Bark, Mark Livelli, Marmar Mehrabadi, Andrea Para, Beth Pavlik, Tamera Scholz, Sarah Shieh and Jason Weaver.

Finally, I would like to thank my family and Jen for their unwavering support.

TABLE OF CONTENTS

ACKNOWLEDGEMENTS	iii
LIST OF TABLES	vi
LIST OF FIGURES	vii
SUMMARY	1
INTRODUCTION	2
Blood Constituents	2
Hemodynamics	2
Arterial Thrombosis	3
Initial Platelet Capture	4
Prior <i>In Vitro</i> Experiments	8
Specific Aims	10
MODEL FOR PLATELET CAPTURE	11
Platelet Bonds	11
Glycoprotein Iba	12
von Willebrand factor	13
Requirements For Platelet Capture	17
Binding Model	24
Ligand Density	30
Receptor Density	31
Contact Percentage	35
Association Rate Constants	38
BINDING SIMULATION METHODS	41
RESULTS	44
Number of Bonds vs. Time	44
Time to Form Necessary Bonds vs. Receptor Density	48
Receptor Density vs. Shear Rate vs. On-rate vs. Contact Percentage	52
DISCUSSION	58
Summary of Results	58
vWF Elongation	61
Activated-Platelet Release of vWF	62
Limitations	62
Future Work	64
Implications of Results	65

CONCLUSIONS	66
APPENDIX A	67
MATLAB Simulation Code.....	67
APPENDIX B	70
Binding Time vs. Domain Density Plots	70
REFERENCES	84

LIST OF TABLES

Table 1: Selected on-rates from the literature.....	39
Table 2: Summary of values used in simulations	40

LIST OF FIGURES

Figure 1: Depiction of hemodynamic properties of blood.....	3
Figure 2: Depiction of the formation of a monolayer of thrombus.....	6
Figure 3: Depiction of platelet deposition	7
Figure 4: Blood flowing through glass stenosis.....	8
Figure 5: Depiction of thrombus structure.....	12
Figure 6: Constituents and arrangement of GPIb-V-IX receptor.....	13
Figure 7: Depiction of a vWF dimer.....	14
Figure 8: Illustration of the periodicity of A1 domains	14
Figure 9: vWF configurations as a function of shear rate.....	16
Figure 10: Illustration of a possible configuration of vWF	17
Figure 11: Illustration of forces on a platelet.....	18
Figure 12: Plot of drag force on a platelet versus shear rate.....	19
Figure 13: Illustration of increasing number of bonds.....	20
Figure 14: The number of bonds as a function of shear rate	21
Figure 15: Illustration of a platelet flowing past a binding spot.....	22
Figure 16: Binding time as a function of shear rate.....	23
Figure 17: Depiction of binding volume for a platelet	28
Figure 18: Calculation of A1 domains accessible.....	32
Figure 19: Illustration of globular and elongated vWF	33
Figure 20: Maximum packing density calculation.....	33
Figure 21: Illustration of the effect of elongation and activation	35
Figure 22: Illustration of contact area calculation for globular vWF	36
Figure 23: Illustration of contact area calculation of flat vWF.....	37
Figure 24: Depictions of a platelet contacting various contours.....	38
Figure 25: Simulation flow chart	42
Figure 26: Number of bonds as a function of time $10,000 \text{ s}^{-1}$	44
Figure 27: Number of bonds as a function of time $100,000 \text{ s}^{-1}$	45
Figure 28: Number of bonds as a function of time 50% contact	46
Figure 29: Number of bonds as a function of time 10 domains.....	47
Figure 30: Number of bonds as a function of time 1000 domains.....	48
Figure 31: Illustration of time points used to create binding time	49
Figure 32: Time versus domain density at $10,000 \text{ s}^{-1}$ and 10%.....	50
Figure 33: Time versus domain density at $100,000 \text{ s}^{-1}$ and 33%.....	51
Figure 34: Time versus domain density at $100,000 \text{ s}^{-1}$ and 10%.....	52
Figure 35: Required domain densities at 1% contact.....	53
Figure 36: Required domain densities at 10% contact.....	54
Figure 37: Required domain densities at 33% contact.....	55
Figure 38: Required domain densities at 50% contact.....	56
Figure 39: Time versus domain density at $10,000 \text{ s}^{-1}$ and 1%.....	70
Figure 40: Time versus domain density at $10,000 \text{ s}^{-1}$ and 10%.....	71
Figure 41: Time versus domain density at $10,000 \text{ s}^{-1}$ and 33%.....	72
Figure 42: Time versus domain density at $10,000 \text{ s}^{-1}$ and 50%.....	73

Figure 43: Time versus domain density at 50,000 s ⁻¹ and 1%	74
Figure 44: Time versus domain density at 50,000 s ⁻¹ and 10%	75
Figure 45: Time versus domain density at 50,000 s ⁻¹ and 33%	76
Figure 46: Time versus domain density at 50,000 s ⁻¹ and 50%	77
Figure 47: Time versus domain density at 100,000 s ⁻¹ and 1%	78
Figure 48: Time versus domain density at 100,000 s ⁻¹ and 10%	79
Figure 49: Time versus domain density at 100,000 s ⁻¹ and 33%	80
Figure 50: Time versus domain density at 100,000 s ⁻¹ and 50%	81
Figure 51: Time versus domain density at 500,000 s ⁻¹ and 33%	82
Figure 52: Time versus domain density at 500,000 s ⁻¹ and 50%	83

SUMMARY

Arterial thrombus forms from the capture and accumulation of circulating platelets on a stenosis. As the thrombus grows, the lumen becomes further stenotic producing very high shear rates as the blood velocities increase through the narrowed cross-section. This study explores the molecular binding conditions that may occur under these pathologic shear conditions where circulating platelets must adhere quickly and with strong bonds.

Platelets binding in an arterial stenosis of >75% are subject to drag forces exceeding 10,000 pN. This force can be balanced by 100 simultaneous GPIb-vWFA1 bonds of 100 pN each. The number and density of GPIb on platelets is sufficiently high; however, platelet capture under high shear would require the density of A1 receptors to be increased to over 416 per square micron. A computational model is used to determine platelet capture as a function of shear rate, surface receptor density, surface contact and kinetic binding rate. A1 density could be increased by a combination of vWF events of: i) plasma vWF attach to the thrombus surface and elongate under shear; ii) the elongated vWF strands create a net with 3-D pockets; and iii) additional vWF is released from mural platelets by activation under shear. With all three events, A1 density matches the existing high GPIb α densities to provide sufficient multivalency for capture at 100,000 s⁻¹ with greater than 170 bonds per platelet. If the on-rate is greater than 10⁸ M⁻¹s⁻¹, then a platelet could be captured within 15 microseconds, the amount of time available to form bonds before the platelet is swept away. This mechanism of platelet capture allows for the rapid platelet accumulation in atherothrombosis seen clinically and in high shear experiments.

INTRODUCTION

Blood Constituents

Blood can be separated into two separate parts: plasma and blood cells. The plasma consists primarily of water but also carries proteins (such as von Willebrand factor and fibrinogen), albumin, electrolytes and dissolved nutrients, to name a few. The cells that are suspended in the plasma fluid are primarily red blood cells, platelets and leukocytes. Nearly all of the cells in the blood are red blood cells; this plays an important role in how the different cells distribute themselves throughout the flowing blood. Red blood cells are, roughly, 7-micron biconcave disc-shaped cells. Platelets can take a variety of shapes and sizes, but measure only, roughly, 3 microns in diameter. Leukocytes measure larger than red blood cells at, roughly, 10 microns in diameter. The size and population of red blood cells causes the smaller and sparser platelets to be pushed to the walls of the blood vessel while under flow, a phenomenon that will be discussed later.

Hemodynamics

Blood flow, in bulk, is modeled as a typical fluid using the laws of Navier-Stokes; however, its particulate nature can make this approximation inaccurate. In this study, blood flow will be considered on a single platelet scale near the wall. On such a small scale the effect of the particulate nature of the fluid can be neglected and blood can be modeled as a fluid creating a linear velocity profile as seen in Figure 1.

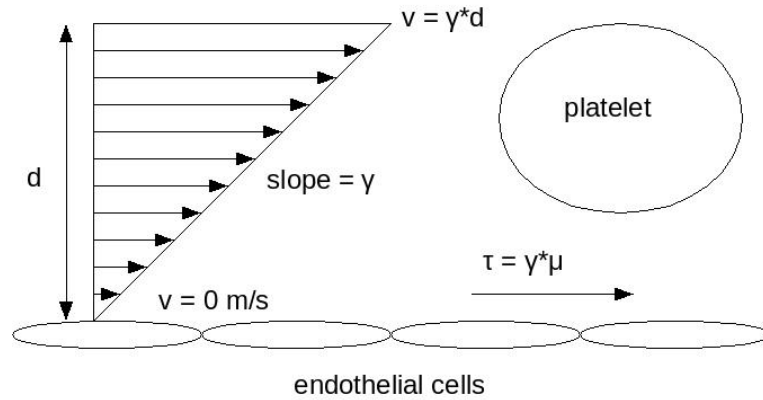


Figure 1: Depiction of hemodynamic properties of blood as considered in this study, where d is the distance from the wall, μ is the fluid viscosity, γ is the shear rate, and τ is the shear stress exerted by the fluid. The platelet is drawn to scale at $\sim 3 \mu\text{m}$ in diameter.

Arterial Thrombosis

Thrombosis, evolutionarily, is a mechanism for hemostasis in the human body. When the body stands to lose blood, clots plug the leak through two mechanisms. When blood shear rates are low, as with small cuts, a “red clot” is formed. Low shear blood clotting has been well researched and uses platelet adhesion molecules such as fibrinogen, fibrin and fibronectin to capture red blood cells at the site of injury. Less understood is the process by which the body forms high shear rate clots, or “white clot”. High shear thrombosis was likely intended to prevent massive bleeding in the case of a severe limb, for example. The severed blood vessels constrict creating a narrowed section that induces high blood velocities that can initiate high shear thrombosis. As humans begin to lead more sedentary lifestyles, the probability of a severed artery has declined and high shear thrombosis has become the source of myocardial infarction and stroke [Davies and Thomas, 1984]. As a leading cause of death worldwide,

atherosclerosis can become fatal when a high shear thrombus occludes an artery supplying the brain or heart. Accordingly, there is great incentive to understand the processes of high shear thrombosis.

High shear thrombosis occurs in regions of vasculature where blood shear rates are very high (greater than $1,000 \text{ s}^{-1}$) and is often due to a constriction in the vessel diameter due to atherosclerosis. As the diameter of the blood vessel decreases, blood velocities increase according to the conservation of mass and create high shear rates. *In vitro* studies of high shear thrombosis have shown that clots, or “thrombi”, tend to deposit throughout the regions of elevated shear [Ku and Flannery, 2007]. As thrombus continues to form on the walls of the constricted section, or “stenosis”, the effective diameter of the blood vessel continues to decrease, further increasing shear rate. Computational analysis has shown that shear rates in *in vitro* models can increase up to $600,000 \text{ s}^{-1}$ [Bark and Ku, 2010]. At such high shear rates near wall ($5 \mu\text{m}$) blood velocities can reach 3 m/s.

Initial Platelet Capture

Platelets originate as cell fragments of megakaryocytes from the bone marrow, break off and enter the blood flow. Platelets can vary in shape and size due to the way they are fragmented. In size, platelets can vary from approximately 2 to 3 microns in diameter when modeled as a sphere [Paulus, 1975]. The shape of a platelet depends on the fluid conditions surrounding it. As shear rate increases, platelets can change from discoid to spherical in shape [Maxwell et al, 2006].

Platelets can adhere to a number of adhesion molecules that allow a platelet to be captured to a blood vessel wall. Collagen, which is exposed at sites of vessel wall endothelial cell injury, binds to glycoprotein IV, glycoprotein VI and integrin $\alpha_2\beta_1$ on the platelet's surface [Ruggeri and Mendolicchio, 2007]. Fibrin/Fibrinogen, which is present on the surface of low shear thrombus, binds to integrin $\alpha_{IIb}\beta_3$ [Ruggeri and Mendolicchio, 2007]. von Willebrand factor, which is present in plasma and released from activated platelets, binds to the glycoprotein Iba receptor on platelets and is the primary adhesion molecule for high shear platelet capture [Ruggeri and Mendolicchio, 2007]. Platelet glycoprotein Iba binds to the A1 receptor on the von Willebrand factor protein.

Platelets travel through the vasculature in highest concentration near the vessel walls; this phenomenon is called platelet margination [Zhao, Kameneva and Antaki, 2007]. As they pass by the vessel wall they usually do not come in contact with adhesion molecules. At sites of vascular wall injury adhesion molecules such as collagen, von Willebrand factor (vWF), or fibrinogen could be present. When a platelet from the flow comes in contact with one of these adhesion molecules, it has a certain amount of time to form a bond before the platelet has passed. The bond cannot be formed if the forces imparted on the platelet exceed the strength of bond. The strength of the bond, the force placed on the platelet and the allowable bond formation time will determine if the platelet will be captured from the flow. In certain cases a cell can form a momentary bond with a wall-bound adhesion molecule before breaking free due to excessive force, causing the cell to adhere, break free and adhere repeatedly in a phenomenon called rolling [Yago et al, 2008].

A thin monolayer of platelet deposition occurs at the site of an injury by adhering to exposed adhesion molecules (most likely collagen).

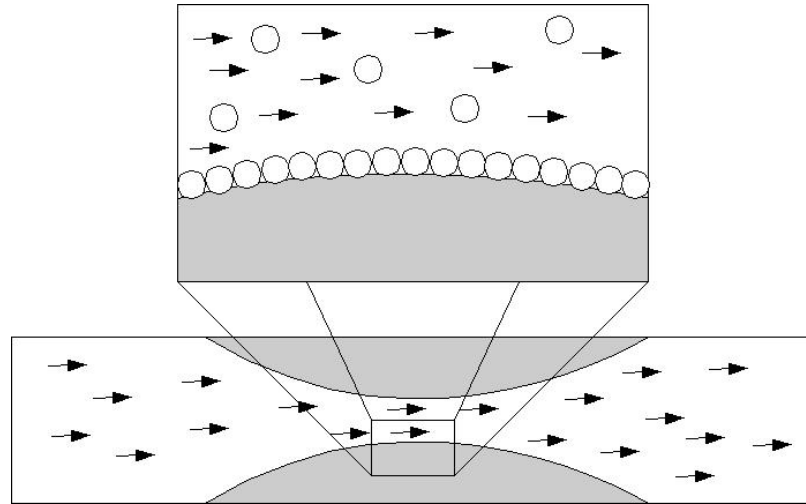


Figure 2: Depiction of the formation of a monolayer of thrombus in a progressive stenosis at high shear. Platelets are represented as spheres for simplicity; platelet shape can vary and would likely be discoid shaped with pseudopod projections.

Once this monolayer forms, inbound platelets are no longer binding to the endothelial wall (or exposed collagen) as it has been covered by platelets. Instead another adhesion molecule (possibly vWF or fibrinogen) must bind platelets to the already-bound platelets. vWF and fibrinogen are present in plasma and can deposit on the surface of the growing thrombus.

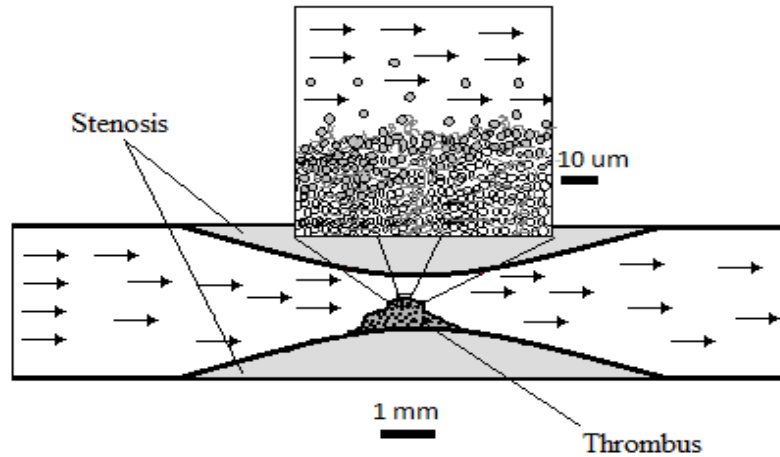


Figure 3: Depiction of platelet deposition to existing thrombus in a progressive stenosis.

Platelets are adhering to other platelets through an adhesion molecule (likely vWF).

Simultaneously, bound platelets are activating (following a delay after initial capture) due to their bound state triggering an activation cascade and the shear force exerted by the moving fluid onto the platelets. Activation causes a number of important processes. The platelets flatten into a discoid shape and pseudopods extend from the membrane. The integrin $\alpha_{IIb}\beta_3$ converts to an activated state allowing firm attachment of the platelet to the thrombus [Ruggeri and Mendolicchio, 2007]. Platelets release a number of signaling chemicals that cause nearby platelets to activate. Platelets release a high concentration of adhesion molecules such as vWF. With firm attachment and high concentrations of vWF and other adhesion molecules, the thrombus surface becomes a firm and sticky surface to capture inbound platelets. This positive feedback loop (bound platelets inducing the binding of more platelets) could be the source of the rapid increases in thrombus growth, dubbed rapid platelet accumulation, that are seen *in vitro* [Ku and Flannery, 2007].

Prior In Vitro Experiments

Prior *in vitro* experimentation conducted in our lab, which was the precedent for this work, demonstrates platelet adhesion under very high shear stresses [Ku and Flannery, 2007]. In these experiments whole porcine blood is flowed through a glass progressive stenosis model. This can be seen in Figure 4.

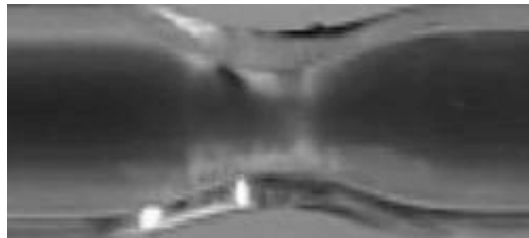


Figure 4: Blood flowing through glass progressive stenosis model. Photo courtesy of
Andrea Para.

An optical microscope equipped with a video camera is used to capture footage of the blood flow at the stenosis. The inside of the glass tubes are coated with collagen to promote initial platelet adhesion. After mural thrombus has been created platelets begin to adhere more rapidly. The thrombus growth continues to occlusion. The camera footage is then analyzed using computational fluid dynamics.

The computational fluid dynamics reveal that shear rates near occlusion can reach $500,000 \text{ s}^{-1}$ with platelet velocities on the order of 1 m/s [Bark and Ku, 2010]. While platelet adhesion cannot be verified at these shear rates, there is measurable thrombus growth at $100,000 \text{ s}^{-1}$ and 1 m/s [Ku and Flannery, 2007]. These increasing shear rates and velocities are contrary to the rapid increases in the ability of platelets to bind to the thrombus surface.

As shear rate increases, along with shear stress and blood velocity, throughout thrombus growth platelets could experience increasing difficulty binding to the thrombus. Increased shear rates impart large forces on the binding platelet requiring that the bond formed between the platelet and the thrombus be very strong. A reasonable platelet bond strength is 100 pN; at a shear rate of $100,000 \text{ s}^{-1}$, a platelet experiences a force of $\sim 10,000$ pN. This would imply that much stronger undiscovered bonds or, more likely, 100 100-pN bonds are necessary to capture a platelet. Increased velocities give the platelet decreasing amounts of time to form bonds with the thrombus surface before they are swept away. For a binding area the size of a platelet ($\sim 1 \text{ } \mu\text{m}^2$), a blood velocity of 1 m/s would only allow $\sim 5 \text{ } \mu\text{s}$ of binding time before the platelet has left the binding area. This would imply that the platelet would need to form ~ 100 bonds in $\sim 5 \text{ } \mu\text{s}$. This conclusion is profound considering the fast rate of bond formation and the lack of precedence for multiple simultaneous bonds in cell adhesion.

Specific Aims

The specific aim of this thesis is to outline a theoretical mechanism to describe high shear platelet capture. The first part of the thesis seeks to quantify the bond force and binding time necessary to capture a platelet as a function of shear rate. As shear rate increases near occlusion, the force imparted on the platelet and the time it has to bind increase and decrease, respectively. In order to counteract the large unbinding forces one possible hypothesis is to invoke multivalent binding. It will be necessary to determine if and how this is possible in the limited time allowed by the increasing platelet velocities. The second part of this thesis will be to develop a quantitative model for the binding reaction between the platelet and the thrombus surface. This will require the modification of existing binding models to apply to the platelet capture reaction. The last part of the thesis will be to describe and quantify the variables that contribute to fast-forming multivalent adhesion between the platelet and the thrombus surface. Finally, the proposed mechanism for high shear platelet capture will be analyzed, discussed and compared to current literature and physiological evidence.

MODEL FOR PLATELET CAPTURE

Platelet Bonds

A thrombus begins often at a site of vascular injury where subendothelium is exposed. Platelets can bind to subendothelium through a variety of adhesion molecules such as: fibrinogen/fibrin, fibronectin, collagen, vWF, laminin, vitronectin, fibulin and thrombospondin. Once the injury site is covered with platelets (this layer is called the mural layer), platelets begin to bind to these bound platelets. When the first layer of platelets binds to the subendothelium, this is referred to as initial adhesion. When platelets begin binding to other platelets, this is called platelet aggregation. This thesis will consider only platelet aggregation, which is the form of adhesion taking place as the thrombus grows to create high shear. At high shear the primary adhesion molecules are vWF and fibrinogen [Ruggeri and Mendolicchio, 2007]. vWF plays a greater role in initial attachment and fibrinogen plays a greater role in stabilization of the thrombus [Ruggeri and Mendolicchio, 2007]. A depiction of the structure of a growing thrombus can be seen in Figure 5.

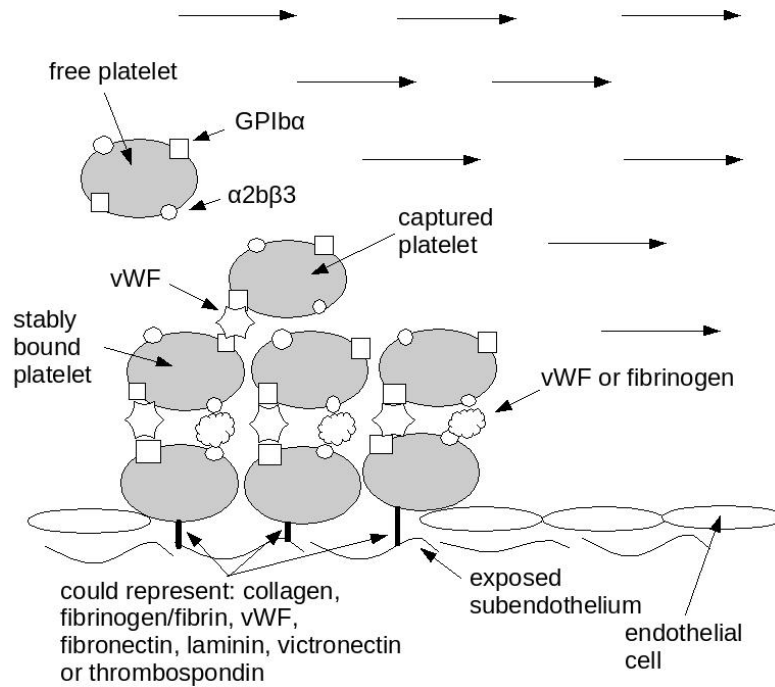


Figure 5: Depiction of thrombus structure and relevant adhesion molecules [Ruggeri and Mendolicchio, 2007].

This thesis is focused on the process of initial platelet capture at high shear; thus, vWF is the only adhesion molecule considered.

The bond created initially between a platelet and vWF is between the glycoprotein Ib α (GPIb α) molecule on the platelet surface and the A1 domain of the vWF protein.

This bond has a strength between 80 and 120 pN [Yago et al, 2008].

Glycoprotein Ib α

GPIb α is a membrane bound receptor found on the surface of a platelet. It is a part of a larger platelet receptor: GPIb-V-IX. This receptor can be seen below.

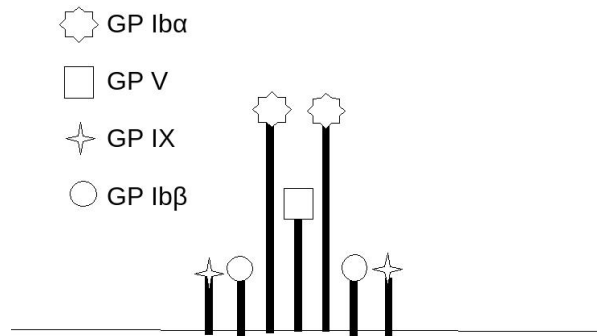


Figure 6: Constituents and arrangement of the GPIb-V-IX platelet receptor [Arya et al, 2005]. Relative heights of receptor components are shown approximately.

GPIb α is the outermost, most accessible portion of the receptor and extends 45 nm from the surface of the platelet [Berndt et al, 1985]. For simplicity, the convention in this paper will be to refer to GPIb α as the “ligand” and vWF-A1 as the “receptor”; the vWF-A1 receptor receives the GPIb α ligand on the inbound platelet.

Multiple GPIb α ligands exist on the surface of a platelet. Berndt et al purified the GPIb α ligand from platelet membranes to determine how many ligands exist on the average platelet surface. The results show that ~23,000 GPIb α ligands exist on a platelet membrane. This plethora of ligands could suggest that multivalent binding between the platelet and vWF could exist.

von Willebrand Factor

von Willebrand factor is a protein synthesized in endothelial cells and platelets. vWF is formed in the ER and Golgi apparatus of these cells, then secreted or stored in either Weibel-Palade bodies (endothelial cells) or α -granules (platelets) [Sadler, 2002]. vWF is comprised of monomers that dimerize to form the repeating unit that builds the

protein [Fowler et al, 1985]. The relative dimensions of the dimer can be seen in Figure 7 [Fowler et al, 1985].

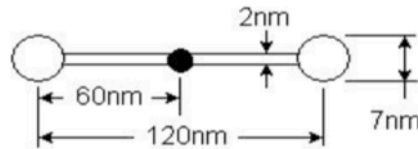


Figure 7: Depiction of a vWF dimer and its relative dimensions [Fowler et al, 1985].

These dimers combine to form long vWF polymers as large as 15 μm in length [Fowler et al, 1985].

The A1 domain of the vWF molecule is located at the globular ends of each monomer. These globular ends are depicted as white circles in Figure 7. On each dimer, the repeating unit of the vWF protein, there are 2 A1 domains. As the dimers assemble into multimers the A1 domains at each end of the dimers come together with a separation of ~ 17 nm [Sadler, 1998]. This creates a pair of A1 domains (~ 17 nm apart) every ~ 120 nm.

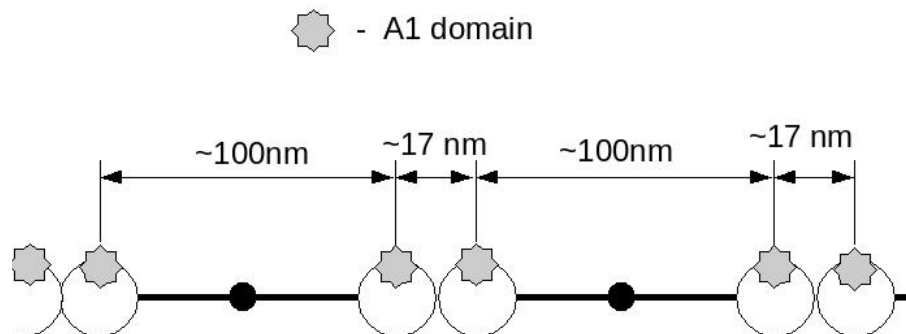


Figure 8: Illustration of the periodicity of A1 domains on the vWF multimer [Fowler et al, 1985].

vWF exists in two configurations: globular and elongated. When vWF is released into the blood stream at low shear stress it assumes a folded tertiary structure [Sadler, 2005]. Once this released vWF experiences high shear stress it unfolds into an elongated tertiary structure. Elongated circulating vWF is cleaved into smaller vWF fragments by enzyme ADAMTS-13 [Zhang et al, 2009, Sadler, 2005]. This is the mechanism behind the heterogeneity of vWF multimer lengths. As vWF has the ability to bind to collagen, platelets, Factor VIII and heparin, it can become immobilized on a thrombus or subendothelial matrix [Sadler, 1998]. When vWF is immobilized it can experience great shear stresses that can cause it to unfold [Ruggeri and Mendolicchio, 2007].

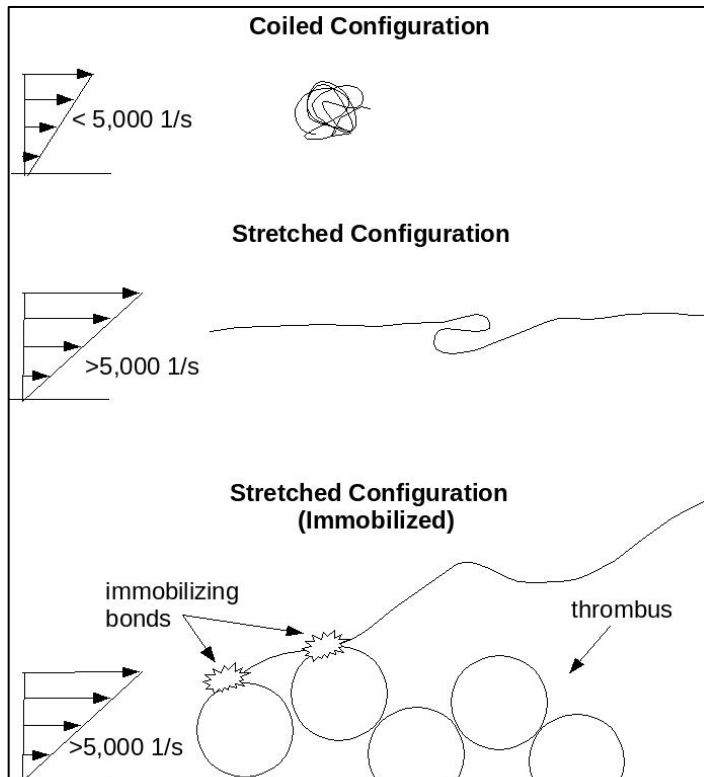


Figure 9: vWF configurations as a function of shear rate [Schneider et al, 2007]. Bottom image depicts possible mechanism of vWF attachment to thrombus.

Thrombus vWF comes from three main sources: blood plasma, α -granules of platelets, and endothelial cells. The vWF from endothelial cells contributes to the mural layer of thrombus as seen in Figure 5; thus, it is not relevant to platelet capture in aggregation. Circulating plasma vWF comes in a variety of sizes as it has been cleaved by ADAMTS-13 and exists at a concentration of 0.01 mg/mL [Harrison and Cramer, 1993]. Plasma vWF can be in its globular or elongated form and has the ability to become immobilized on any blood-contacting surface for which it has receptors. vWF from platelet α -granules is usually released upon activation and exists at a concentration of 0.5 mg/mL [Harrison and Cramer, 1993]. Since there is a much higher concentration

of vWF inside platelets and since platelet activation and vWF release occur at the thrombus surface, platelets are the most relevant source of vWF to high shear platelet capture in aggregation.

vWF can self-associate [Savage, Sixma and Ruggeri, 2002]. This means that vWF can accumulate on the surface of a thrombus even after other vWF molecules consume platelet-binding ligands. vWF can bind to other vWF molecules to form dense protein networks with a high affinity for platelets [Schneider et al, 2007].

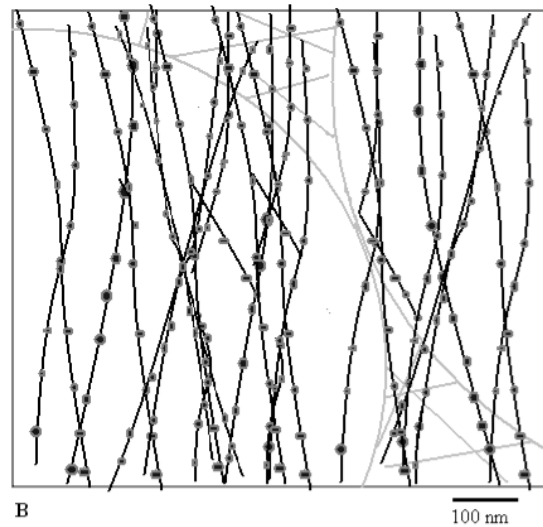


Figure 10: Illustration of a possible configuration of vWF molecules on the surface of a thrombus, forming a dense protein network. Dots represent A1 domains.

Requirements for Platelet Capture

In order to arrest a platelet from the blood flow the platelet must be quickly and strongly associated to the thrombogenic surface. “Quick” and “strong” depend primarily on the shear rate of the blood flow.

To capture a platelet, first, the bond between the platelet and the surface must be strong enough to resist unbinding forces. The primary unbinding force on an arrested platelet is from the blood flow. We will assume that blood flow near the wall can be approximated as Couette flow; this creates a linear velocity profile. The viscosity of the fluid imposes a shear stress on the platelet.

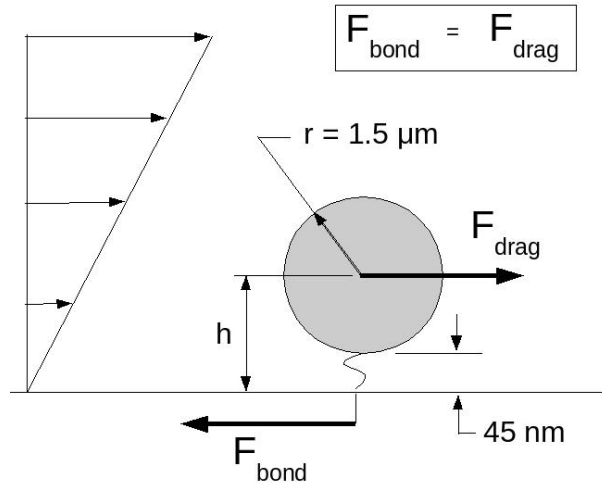


Figure 11: Illustration of forces on a platelet attached to a surface by a GPIIb/IIIa-vWF-A1 with dimensions.

Maxwell et al have determined platelet shape to be a function of shear rate. They find that at shear rates greater than $10,000 \text{ s}^{-1}$ the majority of platelets assume a spherical shape [Maxwell et al, 2006]. Goldman et al have calculated Couette flow past an immobilized sphere to produce the following relationship:

$$F_{\text{platelet}} = 6\pi\mu r h S, \quad (1)$$

where μ is the viscosity of blood, r is the radius of the platelet, h is the distance from the wall to the center of the platelet, and S is the shear rate [Goldman et al, 1967]. The viscosity of blood near the wall is not precisely known [Ku, 1997]. Blood is a particulate fluid, which gives it non-Newtonian properties; viscosity decreases with increasing shear stress [Galdi et al, 2008]. However, in most arteries blood behaves as a Newtonian fluid [Ku, 1997]. We use a viscosity of whole blood, μ , of 4 mPa·s [Ku, 1997]. From the Maxwell et al study of platelet shape as a function of shear rate, we use a spherical platelet radius, r , of 1.5 μm [Maxwell et al, 2006]. The distance between the wall and the center of the platelet, h , is the platelet radius plus the length of the GPIIb/IIIa ligand binding it to the wall, or 1.545 μm . We examine the force on the platelet over a range of pathological shear rates. For the lower end of the range we use 1,000 s^{-1} [Kroll et al 1996]. For the upper end of the range we use 500,000 s^{-1} [Bark and Ku, 2010]. Forces over this range of shear rates can be seen below.

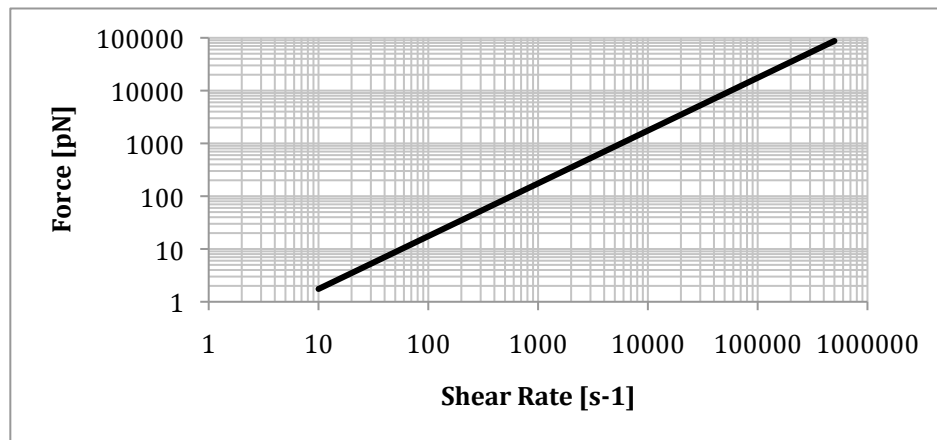


Figure 12: Plot of drag force on a platelet versus shear rate.

Platelet capture has been demonstrated at shear rates as high as $100,000 \text{ s}^{-1}$ [Ku and Flannery, 2007]. Shear rates near occlusion have been shown to reach $500,000 \text{ s}^{-1}$, but platelet capture has not been demonstrated at this shear rate [Bark and Ku, 2010]. The strength of a single GPIIb/IIIa-vWF-A1 is 100 pN [Yago et al, 2008]. As can be seen in Figure 11, the drag force on a platelet exceeds 100 pN at $\sim 600 \text{ s}^{-1}$, continuing to $\sim 17,000$ pN at $100,000 \text{ s}^{-1}$. Considering that the GPIIb/IIIa-vWF-A1 bond is the bond responsible for platelet capture at high shear, multiple GPIIb/IIIa-vWF-A1 bonds must be created to resist the drag forces placed on the platelet above $\sim 600 \text{ s}^{-1}$.

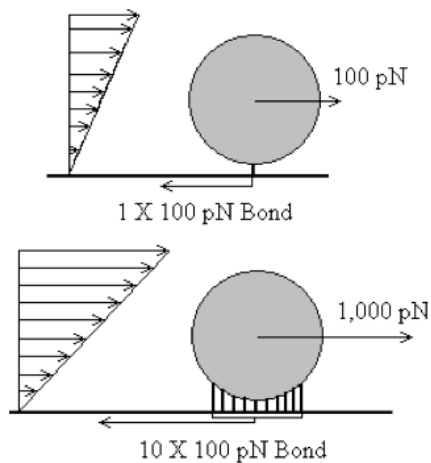


Figure 13: Illustration of increasing required number of bonds.

A plot of the number of bonds that are required at a given shear rate can be derived from Figure 13 as seen below.

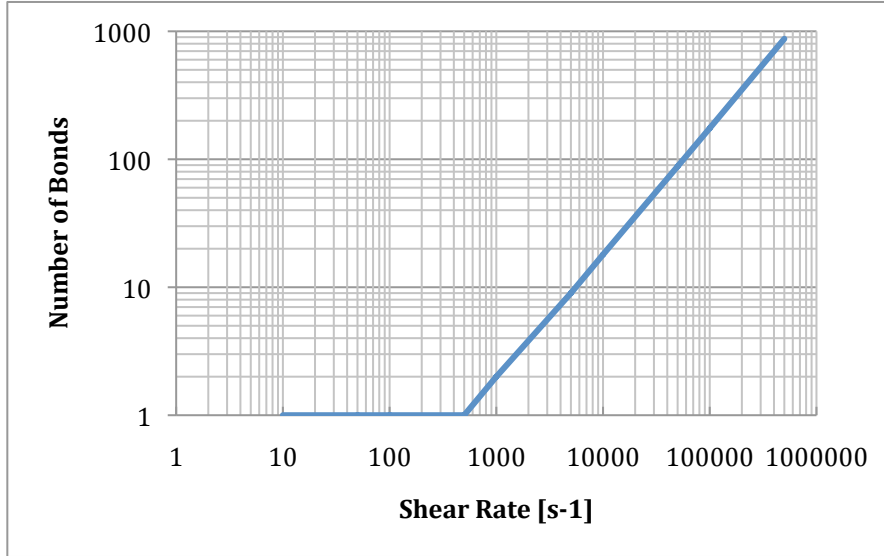


Figure 14: The number of bonds required to capture a platelet as a function of shear rate.

According to Figure 13, ~170 bonds are required to capture a platelet at $100,000 \text{ s}^{-1}$. This is a large number of bonds to form quickly.

Secondly, in order for a platelet to be captured from the flow, the appropriate number of bonds must be formed before the platelet is swept away by the flow. The velocity of a platelet near the vessel wall can be approximated from the shear rate. An inbound platelet will travel approximately $5 \mu\text{m}$ from the wall before it is captured. At this distance the velocity of the platelet can be approximated using the following formula:

$$v_p = Sd, \quad (2)$$

where v_p is the velocity of the platelet, S is the shear rate and d is the distance from the vessel wall (where d is $\sim 2 \mu\text{m}$, or one platelet radius). Using the platelet velocity we can

determine the amount of time the platelet has to bind to the thrombogenic surface by assuming a distance over which the platelet can bind.

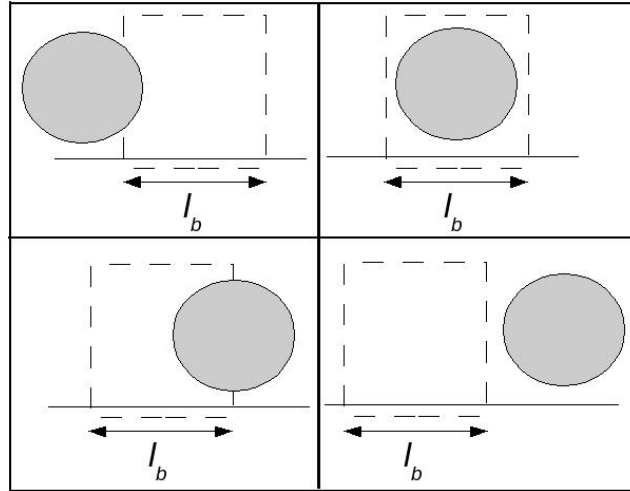


Figure 15: Illustration of a platelet flowing past a binding spot.

Once the platelet flows past this binding spot, it can no longer bind. This concept is con be written as follows:

$$t_b = l_s/v_b, \quad (3)$$

where t_b is the allowable binding time, l_s is the length of the binding spot and v_b is the platelet velocity. We use a binding spot length, l_s , of approximately one platelet diameter or $3\mu\text{m}$. By combining Equation (2) and Equation (3) and substituting known values (l_s and d), we obtain the following relationship between binding time, t_b , and shear rate, S :

$$t_b = 1.5/S. \quad (4)$$

We plot the above equation to obtain Figure 15, demonstrating the allowable binding time at a given shear rate.

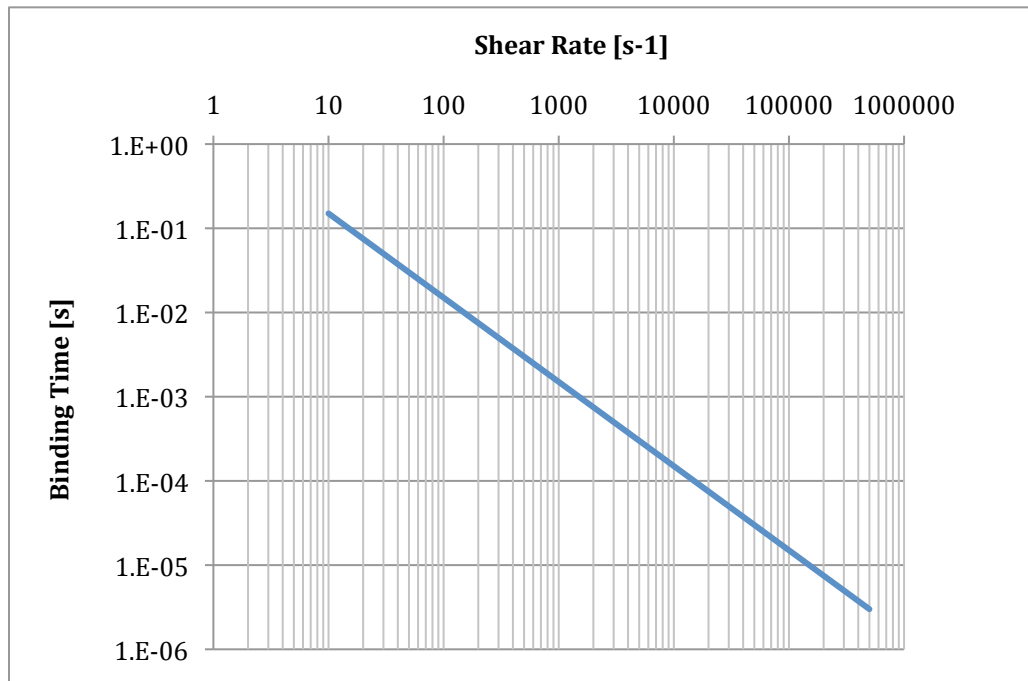


Figure 16: Binding time as a function of shear rate.

From Figure 15 we can see that at $100,000 \text{ s}^{-1}$, a platelet has 15 microseconds to form a stable bond with the thrombus surface. As mentioned earlier, ~ 170 bonds are required to arrest a platelet at $100,000 \text{ s}^{-1}$; this means that in order for a platelet to be captured at this shear rate, 170 bonds must be formed in 15 microseconds. This is a very fast binding rate; thus, we have developed a model to simulate this binding event and quantify the variables that allow for such a binding rate.

Binding Model

A number of models exist for modeling the adhesion of a convecting cell to a surface. While these models may accurately describe the scenario, they are difficult to use given what has been quantified about the bond in question. The focus of these difficulties is the association and dissociation rate constants.

A valid model for platelet adhesion is the one proposed by Hammer and Lauffenburger in 1987. This model considers a flowing cell with some density of surface ligands contacting a surface with some density of receptors over some known contact area. This model is based on the following equation:

$$dN_b/dt = k_f N_{l0} N_a - k_r N_b, \quad (5)$$

where N_b is the number of bonds per unit area, k_f is the forward rate constant, N_{l0} is the density of ligands on the cell, N_a is the density of receptors on the surface and k_r is the reverse rate constant [Hammer and Lauffenburger, 1987]. This equation is modified to include the effects of cell dimensions, contact area, contact time, ligand movement, bond interaction length and thermodynamics, resulting in the following equation:

$$d\eta_b/d\tau = \theta[\eta_a - \kappa\eta_b \exp(\alpha/\beta R_T \eta_b)], \quad (6)$$

$$d\eta_a/d\tau = \theta[-\eta_a + \kappa\eta_b \exp(\alpha/\beta R_T \eta_b) + \delta(1 - \eta_b)], \quad (7)$$

where η_b is the ratio of the bond density to the initial ligand density, τ is the ratio of time to contact time, θ is the bond formation rate, η_a is the ratio of the free ligand density to

the initial ligand density, κ is the dissociation rate, α is the bond breakage energy, β is the contact area, R_T is the number of ligands and δ is the ligand accumulation rate [Hammer and Lauffenburger, 1987]. This model considers many important elements of platelet capture; however, this model cannot be used to compare values to literature as the on-rate constant on which it is based carries units of cm^2/s while on-rates are typically reported in $1/\text{M}\cdot\text{s}$. On-rate constants are typically determined in an equilibrium reaction with ligands and receptors in solution; thus, molarity is important. Without the ability to compare to literature values, we cannot determine the input value of the on-rate constant and, consequently, we cannot determine the solution to the equation. If on-rate values could be measured in a way more consistent with this model and reported in cm^2/s , then this model would be ideal for describing platelet capture.

Other improved models have been developed since Hammer and Lauffenberger's model in 1987. Hammer and King developed a model in 2001 that considers the geometric alignment of ligands on the cell and receptors on the surface [King and Hammer, 2001]. The model also considers the overlapping of the receptors and ligands. Another model by Krasik, Yee and Hammer in 2006 considers signal transduction upon bond formation, which can allow for the arrest of the cell through integrin activation [Krasik, Yee and Hamer, 2006]. Recently, Yago et al in 2007 consider the probability of a platelet bond forming based on collision frequency, area of contact and the densities of receptors and ligands [Yago et al, 2007]. Each of these studies, as well as a study by Mody and King in 2008, consider platelet bonds as springs that break free as a function of loading rate and other thermodynamic considerations using the Bell model [Mody and King, 2008, Bell, 1978]. The Bell model bond dissociation rate is based on the energy

being placed in the bond. By assuming a fixed dissociation rate and bond strength, our model is simplified, though these values could be changed once the energy is known. Furthermore, Doggett et al in 2002 demonstrated that as force increases on the order of 100 pN, dissociation rate increased on the order of 10^1 s^{-1} [Doggett et al, 2002]. At our greater forces we could expect the dissociation rate to be higher, but not by orders of magnitude. We will instead assume the final bond dissociation force to be a constant $\sim 100 \text{ pN}$ independent of loading rate as loading rate will tend to vary with fluid and surface conditions. Each of the referenced models considers shear rates that are lower (maximum shear rates from $50 - 10,000 \text{ s}^{-1}$) than the shear rates we are considering for this study. These models predict behaviors at lower shear rates that could be relevant to high shear platelet capture. Instead of considering the various phenomena that contribute to the platelet binding strength, we assume a fixed value for the bond strength of approximately 100 pN. The bond strength could be varied in our model based on the loading rate, thermodynamic considerations, or other variables if they are known.

The most essential receptor-ligand binding equation is the equilibrium binding equation. This equation addresses receptor-ligand binding in solution and is shown below:

$$dC_b/dt = k_{on}C_lC_r - k_{off}C_b, \quad (8)$$

where C_b is the concentration of receptor-ligand complexes, k_{on} is the on-rate constant, C_l is the concentration of ligands, C_r is the concentration of receptors and k_{off} is the off-rate constant [Trusky, Yuan and Katz, 2004]. C_l and C_r are the concentrations of ligands and

receptors at a time t . Using initial receptor and ligand concentrations, Equation 8 can be rewritten as follows:

$$dC_b/dt = k_{on}(C_{l0} - C_b)(C_{r0} - C_b) - k_{off}C_b, \quad (8)$$

where C_{l0} is the initial concentration of ligands and C_{r0} is the initial concentration of receptors [Trusky, Yuan and Katz, 2004]. The inputs to this equation are receptor and ligand concentrations and on and off-rate constants. On-rate and off-rate constants are available from previous studies. Receptor and ligand concentrations, however, are not relevant to our binding scenario. Receptors and ligands bound to surfaces and cell membranes are not in solution and, thus, are not easily described with a concentration. In order to use this equation to more accurately describe platelet capture we must interpret bound receptors and ligands as concentrations.

A concentration of receptors or ligands can be determined from the number of receptors or ligands by assuming a volume as follows:

$$C = N/VN_{AV}, \quad (9)$$

where C is the concentration, N is the number of ligands or receptors, V is the volume containing the receptors or ligands and N_{AV} is Avogadro's number [Trusky, Yuan and Katz, 2004]. A volume that best describes the platelet binding reaction must be determined.

The binding reaction between a platelet and vWF-coated surface happens exclusively within the narrow space between the platelet and the surface. A depiction of what this binding volume might look like can be seen in Figure 16.

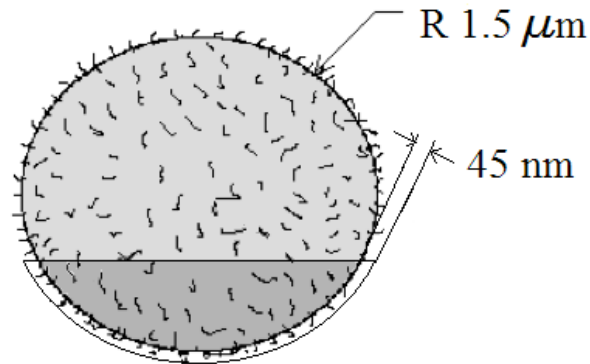


Figure 17: Depiction of binding volume for a platelet contacting a thrombogenic surface with approximately one third of its surface area.

There are a number of receptors on the platelet surface that should not be considered in the binding volume as they are too far from the thrombogenic surface to take part in the reaction; therefore, it is necessary to define which receptors can be included in the binding volume; this will be handled explicitly in a later section. Accordingly, the binding volume can be defined to include the surface area of the platelet that can be involved in the binding reaction; this area is shown in grey in Figure 16. A third dimension is required to determine the binding volume. We will assume the binding volume extends 45 nm , or the length of a GPIIb/IIIa ligand, away from the surface of the platelet as shown in Figure 16. The binding volume, V , can be calculated using the following equation:

$$V = Ah = 4\pi r^2 Ph, \quad (10)$$

where A is the area of contact between the platelet and the thrombogenic surface, h is the height of a GPIIb/IIIa ligand (45 nm), r is the platelet radius and P is the platelet contact percentage. Instead of considering exact platelet contact areas, we will examine a few platelet contact percentages, or the percentage of platelet surface area that is within binding range of the surface. Substituting Equations (9) and (10) into Equation (8) gives the following equation:

$$dN_b/dt = k_{on}(N_{l0} - N_b)(N_{r0} - N_b)/(VN_{AV}) - k_{off}N_b. \quad (10)$$

The numbers of receptors and ligands involved in the binding reaction depends on the density of receptors and ligands on the surfaces and the area over which they contact each other. Accordingly, Equation 10 must be modified to more accurately describe this interaction. The number of receptors can be written as follows:

$$N = \phi A = \phi P 4\pi r^2, \quad (11)$$

where N is the number of receptors or ligands and ϕ is the density of receptors or ligands on the platelet or thrombus surface. Substituting Equation 11 into Equation 10 gives the following differential equation:

$$dN_B/dt = (4\pi r^2 P k_{on}/hN_{AV})(\phi_R - N_B/4\pi r^2 P)(\phi_L - N_B/4\pi r^2 P) - k_{off}N_B. \quad (12)$$

Equation 12 is the differential equation with which the platelet binding reaction will be modeled. The number of bonds formed in a given amount of time can be determined by solving Equation 12 for various contact percentages, P , rate constants, k_{on} and k_{off} , receptor densities, ϕ_R , and ligand densities, ϕ_L . Knowing the number of bonds formed in a given amount of time, we can determine if platelet capture is possible using Figure 13 and Figure 15.

Ligand Density

The density of GPIb α ligands on the surface of a platelet is a relatively fixed quantity. Though ligands are capable of diffusing in the cell membrane, this process is too slow for the capture events at very high shear. Cell surface receptor mobility diffusion rates are on the order of 10^{-9} cm²/s [Schlessinger et al, 1976]. As binding occurs on the order of microseconds we can calculate how far a ligand could diffuse across the platelet surface in 10 microseconds. With a diffusion rate of 10^{-9} cm²/s and a time of 10^{-5} s, a ligand could travel approximately 1 nm. A nanometer of diffusion would not effect the distribution of ligands on the surface of the platelet significantly and thus we assume the ligand density to be fixed. A study by Dong et al in 1997, suggests that the GPIb-IX complex has restricted mobility to allow the ligand position to remain fixed for better geometric alignment with vWF [Dong et al, 1997].

As GPIb α ligands are essentially fixed, the relative positioning of the vWF-A1 domains governs the steric alignment of the GPIb α and vWF-A1 for bond formation. This is analogous to Velcro [U.S. Patent No. 2,717,437]. One surface of Velcro has

ordered, fixed, evenly spaced hooks (analogous to GPIb α ligands) while the other surface can be randomly ordered, is not fixed, dense (analogous to vWF). The steric alignment of receptors and ligands thus becomes less important as the randomly located A1 domains become denser.

In a 1985 study Berndt et al radio labeled and counted the GPIb α molecules on the surface of a platelet. Berndt et al examined data from 7 platelets to determine that these platelets carried ~23,000 GPIb α molecules on their surfaces. This number varied by ~10%; as platelet size varies, this would suggest that the density of domains on a platelet would remain relatively constant. Considering our earlier determined platelet dimensions ($r = 1.5 \mu\text{m}$), and assuming an even distribution of GPIb α ligands on the surface of the platelet, this gives a ligand density of ~800 GPIb α ligands per square micron. This number will remain fixed throughout our simulations as the ligand density will likely remain unchanged for a particular platelet.

Receptor Density

As the binding surface is created by vWF binding to the thrombus surface, the density of receptors varies with the amount of vWF on the surface and the availability of its A1 domains. In order to determine the range of receptor densities we must consider the shape of vWF. vWF on the thrombus surface can be in its globular or elongated form. In its globular form, a 15 micron vWF protein can be modeled as a 1 micron diameter sphere [Schneider et al, 2007]. Elongated vWF can be modeled as a strand, which can then form many different contours. We can determine the maximum vWF-A1 receptor density by determining the maximum number of exposed A1 domains we can fit

in a given area. Considering a 1 square micron area, we calculate the maximum number of A1 domains that can exist with vWF in its globular or elongated form.

Globular vWF approximately assumes the shape of a sphere. This shape takes up a large amount of space with a low surface area. Many of the A1 domains of the vWF protein in the sphere are inaccessible. To determine how many A1 domains are available we assume the A1 domains of the 15 μm vWF protein that makes up the sphere are evenly distributed within its volume. This is illustrated in Figure 17.

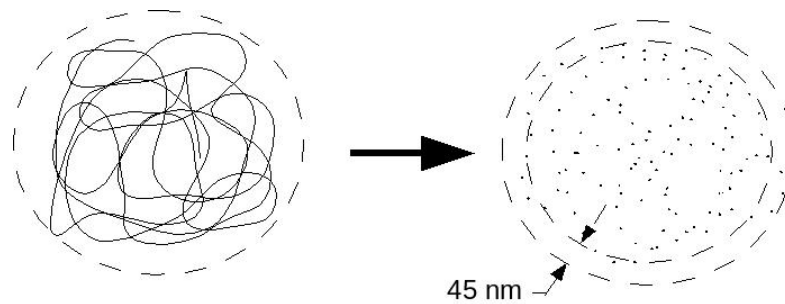


Figure 18: Calculation of A1 domains accessible by platelet ligands.

As vWF has 1 A1 domain every 120 nm, we can assume that a 15 μm long vWF protein has 125 A1 domains. If we distribute these domains over the $5.24 \times 10^{-19} \text{ m}^3$ volume of the globular vWF protein, we obtain a volumetric density of 2.39×10^{20} A1 domains/ m^3 . If we consider only the A1 domains that are accessible by the GPIb α molecule, then we can only consider the first 45 nm of volume from the surface of the sphere (Figure 17). This layer is $\sim 1.29 \times 10^{-19} \text{ m}^3$ and, thus, contains ~ 31 A1 domains. If we distribute these 22 domains over the surface of the sphere, that gives a receptor density of ~ 10 domains per square micron. As only one globular vWF protein can fit in a square micron, there is a single value of domain densities for globular vWF (or none). In elongated form,

multiple vWF strands can occupy the square micron area simultaneously (Figure 18); thus, for elongated vWF we must consider a range of densities.

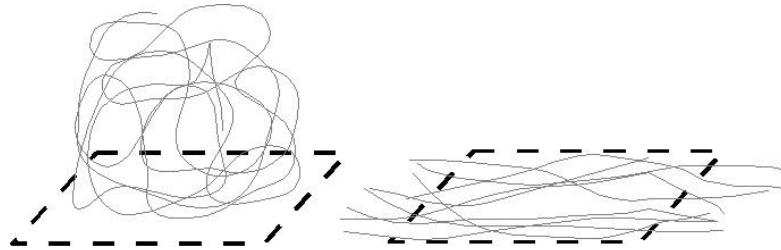


Figure 19: Illustration of globular and elongated vWF and 1 square micron area.

In order to determine the maximum domain density for elongated vWF we must calculate the maximum number of vWF strands that can fit in a square micron. If we assume that vWF proteins can lie directly next to each other without interference effects, we can calculate the close-packed density of elongated vWF from the dimensions given in Figure 8. If we align vWF molecules as close together as possible (as depicted in Figure 19) we can fit one vWF protein every 4.5 nm.

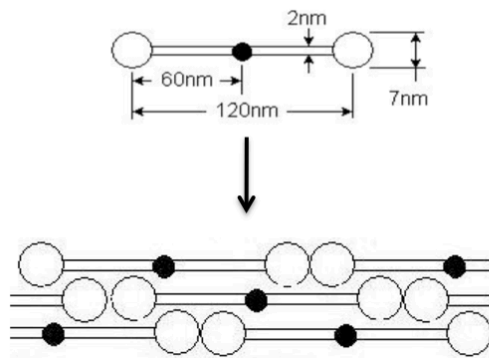


Figure 20: Maximum packing density calculation for elongated vWF

With one vWF strand every 4.5 nm, we can fit 222 strands widthwise in a square micron. Since there is one A1 domain every 120 nm lengthwise, there are 12 domains per strand in a micron of length. This gives 2664 domains per square micron as the maximum domain density for elongated vWF. This configuration is unlikely to form naturally and merely bounds a range of domain densities to test in the simulation. The range for domain density of elongated vWF is thus 0 – 2664 domains per square micron.

To determine the effects of vWF concentrations released due to platelet activation, we calculated the domain density created by such a concentration. vWF exists in plasma at a concentration of 0.01 milligrams per milliliter within an α -granule of a platelet at a concentration of 0.5 milligrams per milliliter. This converts to 1×10^{13} and 6×10^{14} vWFA1 domains per milliliter respectively. These concentrations can be converted to planar vWFA1 densities yielding densities of 1 domain per square micron for plasma vWF concentrations and 50 domains per square micron for activated-platelet-released vWF concentrations. This suggests that activation is likely for receptor densities greater than 50 domains per square micron. These values assume that the platelets release their entire α -granule contents and that all vWF present adheres to the aggregate. These densities can also increase since upstream vWF can accumulate on the aggregate surface downstream over time. The effects of elongation and activation are illustrated in Figure 20.

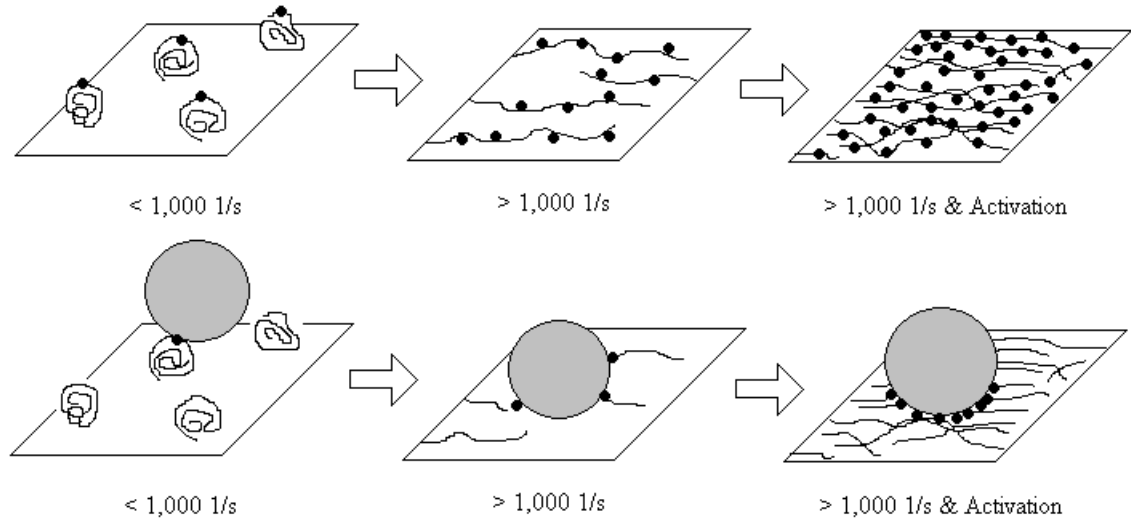


Figure 21: Illustration of the effect of elongation and activation on receptor density and binding strength. Shear rates listed are approximate. vWF unfolds between $1,000 \text{ s}^{-1}$ and $6,000 \text{ s}^{-1}$ [Schneider et al, 2007].

Contact Percentage

The percentage of the platelets surface area that comes in contact with the thrombogenic surface depends on the shape of the surface relative to the shape of the platelet. The surface contour is determined by the platelets that make up the thrombus and the vWF (and other molecules) that lay on top of them. We assume that the top-most layer of platelets creates the backbone of the thrombus contour and the vWF that lies on top of it creates the detailed features of the thrombus contour. Since we assume that platelets are only binding to surface vWF at high shear, we can assume that the binding platelets that we are concerned with are only contact vWF covered surfaces.

Since the shape of vWF determines the contour of the platelet-binding surface we must consider its shape. Each conformation of vWF creates a different area of contact with the binding platelet. To determine the contact percentage that we use in the binding

simulation we must determine the contact area between a platelet and the various possible vWF contours.

Globular vWF most likely presents a concave binding surface to a binding platelet. The extent of this concavity can vary with the shape of the vWF globule. We model globular vWF as a 1 micron diameter sphere and, thus, for our model we use a single value for the platelet contact percentage of globular vWF. To calculate this value we need to determine the contact area between two spheres (the platelet and the vWF) of different radii. The area of contact is determined by calculating the area of the platelet that is within one GPIIb/IIIa molecule length (45 nm) of the globular vWF. This calculation is illustrated in Figure 21.

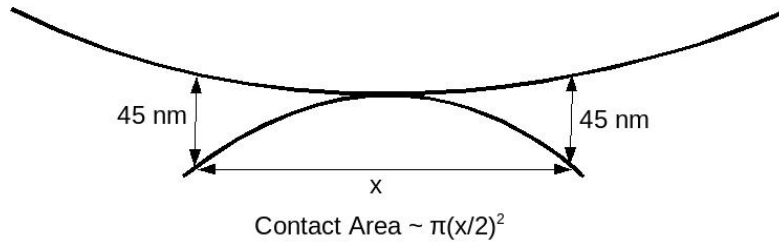


Figure 22: Illustration of contact area calculation for globular vWF.

In order to calculate x as seen in Figure 21, we use the following equation:

$$0.045 = R_{platelet} - \sqrt{R_{platelet}^2 - (x/2)^2} + R_{vWF} - \sqrt{R_{vWF}^2 - (x/2)^2}, \quad (13)$$

where $R_{platelet}$ is the radius of the platelet and R_{vWF} is the radius of the vWF globule. We use a platelet radius of 1.5 μm and a vWF radius of 0.5 μm . Solving the equation for x

gives a value of 0.362. This gives a contact area of $0.1 \mu\text{m}^2$ or 0.7 % of the platelet surface area. Thus, the platelet contact percentage for globular vWF is $\sim 0.7\%$.

Elongated vWF can assume nearly any contour. We assume that it is likely to conform to the surface to which it is bound. The thrombus surface can achieve maximum platelet contact with a pocket. The maximum contact percentage this pocket could have with the platelet is 50%. If the pocket were any more curved, the platelet would not be able to enter. Thus the maximum platelet contact percentage for elongated vWF is 50%.

We have also calculated the contact percentage created by a flat surface. This is illustrated in Figure 22.

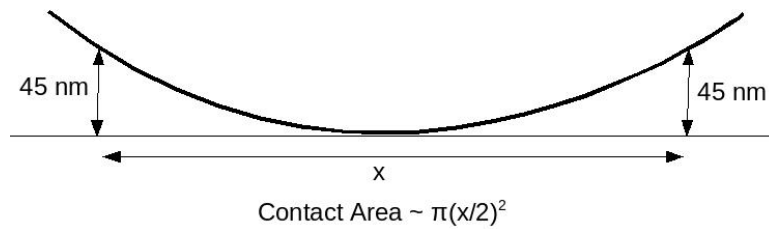


Figure 23: Illustration of contact area calculation of flat vWF.

In order to calculate x as seen in Figure 22, we use the following equation:

$$0.045 = R_{platelet} - \sqrt{(R_{platelet}^2 - (x/2)^2)}. \quad (14)$$

Solving the equation for x gives a value of 0.792. This gives a contact area of $0.4 \mu\text{m}^2$ or 3 % of the platelet surface area. Thus, the platelet contact percentage for flat vWF is $\sim 1\%$.

In our simulation we consider a few sample contact percentages: 0.7% (globular), 1% (flat), 10%, 33% and 50%. Figure 23 illustrates how surface contour can affect platelet contact percentage.

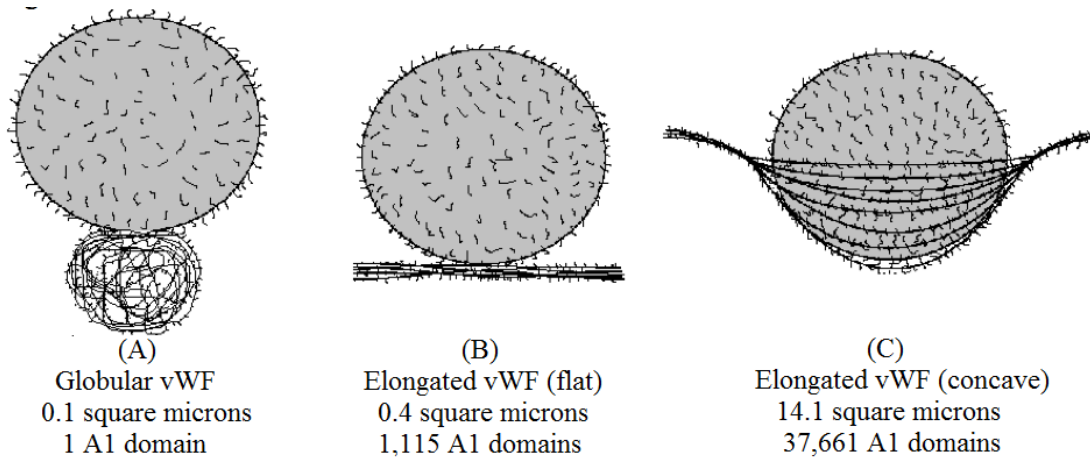


Figure 24: Depictions (profile view) of a platelet contacting various contours of a vWF surface: (A) a 1 μm diameter sphere of globular vWF, (B) a flat elongated vWF and (C) a maximally concave elongated vWF (50% of platelet surface contacted). Listed below each are the maximum contact area and the maximum number of domains that can be contacted (using a receptor density 2664 domains per square micron)

Association Rate Constants

The off-rate constant for a GPIIb α -vWF-A1 bond has been calculated in a number of studies yielding a value of roughly 5 s^{-1} [Miura et al, 2000, Doggett et al, 2003, Kumar et al, 2003]. Investigations of the on-rate constant have produced varying results [Kumar et al, 2003]. In two different studies researchers used the dissociation concentration along with the previously mentioned off-rate measurements to estimate two different on-rates: 10^3 and $10^5 \text{ M}^{-1}\text{s}^{-1}$ [Miura et al, 2000, Mody and King, 2008]. A common analogue

for platelet binding, leukocyte capture by selectins, suggests that the on-rate may be closer to $10^6 \text{ M}^{-1}\text{s}^{-1}$ [Mehta, Cummings and McEver, 1998]. The range of values for each of these kinetic rates is difficult to determine experimentally; thus, we vary the kinetic on-rate, k_{on} , and determine what values can provide a plausible solution. In our simulations, we consider a range of on-rates from 10^3 - 10^{10} , based on other biological bonds (Table 1).

Table 1: Selected on-rates from the literature.

	On Rate Constant [$\text{M}^{-1} \text{s}^{-1}$]	Binding Process
Inter-cellular	10^3	vWF/GPIb on-rate [Miura et al, 2000]
	10^5	vWF/GPIb on-rate [Mody and King, 2008]
	10^6	SPR-determined Leukocyte/Selectin on-rates [Mehta, Cummings and McEver, 1998, Nicholson et al, 1998]
Intra-cellular	10^6	Actin filament assembly [Salmon, McKeel and Hays, 1984]
	10^{10}	Myosin/Actin [Marston, 1982]

We assume that on-rate and off-rate do not vary with shear rate, as these are considered quasi-static equilibrium kinetic reactions. In the case of the off-rate constant, this assumption appears justified [Doggett et al, 2003].

Table 2: Summary of values used in simulations

Variable	Symbol	Value
GPIb α Density	ϕ_L	800 μm^{-2}
vWF-A1 Density (Globular)	ϕ_R	0-10 μm^{-2}
vWF-A1 Density (Elongated)	ϕ_R	0-2664 μm^{-2}
Off-rate constant	k_{off}	5 $\text{M}^{-1}\text{s}^{-1}$
On-rate constant	k_{on}	10^6 - 10^9 $\text{M}^{-1}\text{s}^{-1}$
Platelet contact percentage	P	0.4% (glob.), 1% (flat), 10%, 33%, 50% (concave)

BINDING SIMULATION METHODS

In order to determine the effect of each variable on the ability for a platelet to be captured from a high shear flow, a simulation was developed using MATLAB (MathWorks, Natick, MA). The output of the simulation is a plots showing the relationship between receptor density and the time it takes to form the required number of bonds for different shear rates, contact percentages and on-rates. This is accomplished by iteratively solving Equation 12 over a range of inputs and extracting key data points. The simulation used here uses Equation 10 for simplicity; Equation 12 can be used for a more straightforward, non-iterative calculation.

For a given set of inputs, Equation 10 is solved to give the number of bonds formed as a function of time. This set of data is then analyzed to determine at what time point the appropriate number of bonds, for the given shear rate (Figure 13), is formed. This time point is then assigned to the receptor density used to solve Equation 10. This process is iterated for the full range of shear rates, on-rates and receptor densities. A figure illustrating the block diagram of the simulation can be seen below (Figure 20).

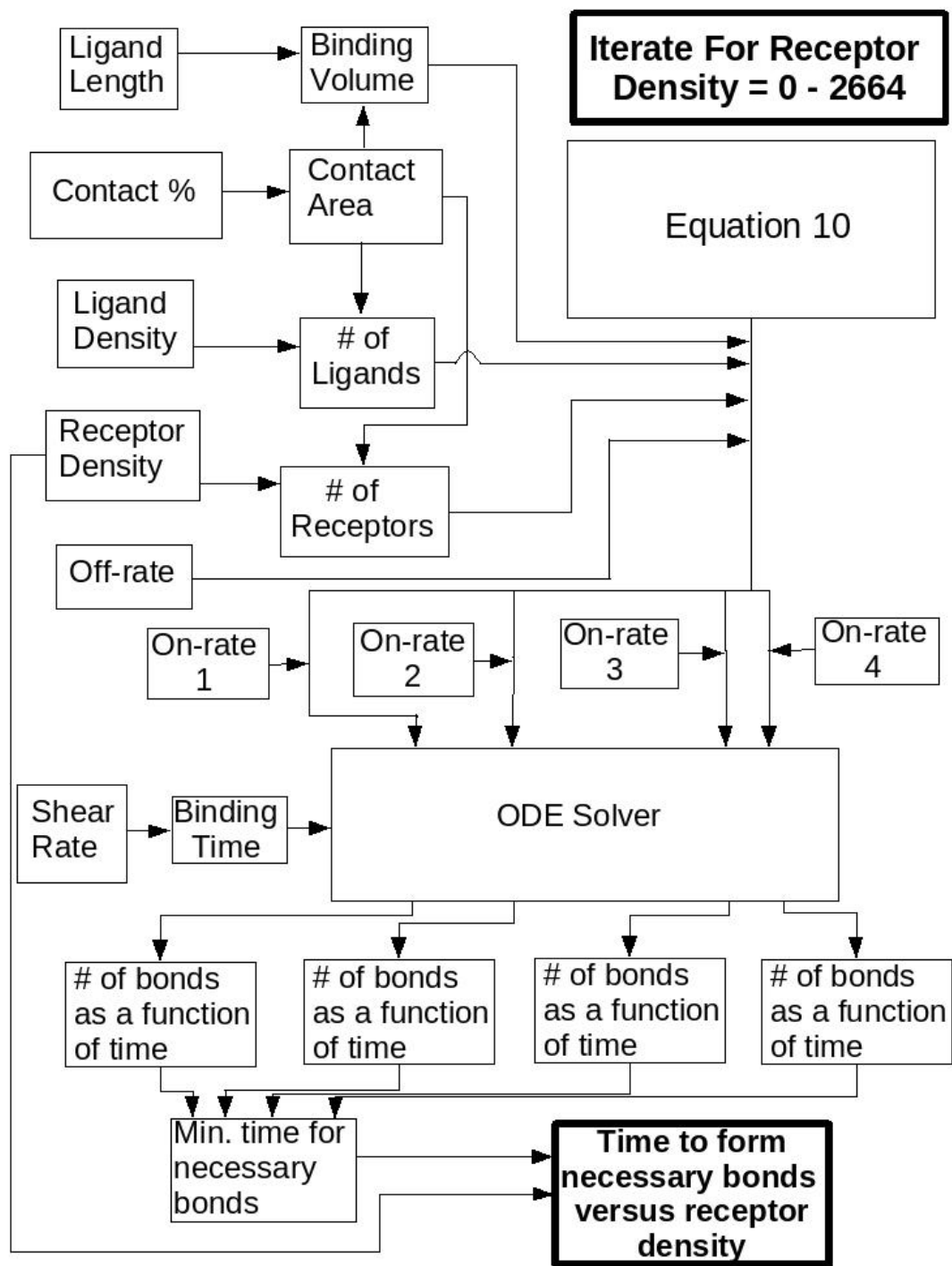


Figure 25: Simulation flow chart.

The simulation begins with 10 inputs: shear rate, length of the ligand, contact percentage, ligand density, range of receptor densities, first selected on-rate, second on-rate, third on-

rate, fourth on-rate and off-rate. Each iteration of the process depicted in Figure 20 uses a different receptor density from the 0 to 2663 domains per square micron. The shear rate, S , is used to calculate the number of bonds necessary to capture the platelet, b , and the binding time, t_b . The contact percentage, P , is used to determine the area of contact between the platelets, A . The ligand length, h , is then used with the contact area to determine the binding volume, V . The ligand density, ϕ_L , and the contact area are used to determine the number of ligands involved in the reaction, N_{l0} . The particular receptor density of a given iteration, ϕ_R , and the contact area are used to calculate the number of receptors used in that iteration, N_{r0} . The off-rate, k_{off} , the number of ligands, the number of receptors and the binding volume are then substituted into Equation 10. Equation 10 is then solved over the time span (0 to t_b) four different times using four different on-rates, k_{on1} , k_{on2} , k_{on3} , k_{on4} , chosen from Table 1. The solutions, the number of bonds as a function of time, for each on-rate (4 solutions) are then analyzed to find the time point at which the appropriate number of bonds is reached. These time points are assigned to their designated on-rate and receptor density in a matrix. The process is then repeated for the next receptor density. Once all iterations are complete, the resulting matrix is converted into plot of the time to form the necessary number of bonds versus receptor density. Full detailed MATLAB code for this simulation can be found in Appendix A.

The simulation is run for a series of shear rates and contact percentages by hand (as opposed to another iterating loop). After examining the resulting plots of each combination minimum receptor densities for capture are paired with their particular shear rate, on-rate and contact percentage. These data are then presented in four 3-D plots (receptor density vs. shear rate vs. on-rate), one for each platelet contact percentage.

RESULTS

Platelet Bonds as a Function of Time

The first result produced by the simulation is the number of bonds formed as a function of time for various shear rates and on-rates. For each iteration the simulation creates a sample bonds-versus-time plot for a particular receptor density. This particular receptor density can be set within the code before the simulation is run.

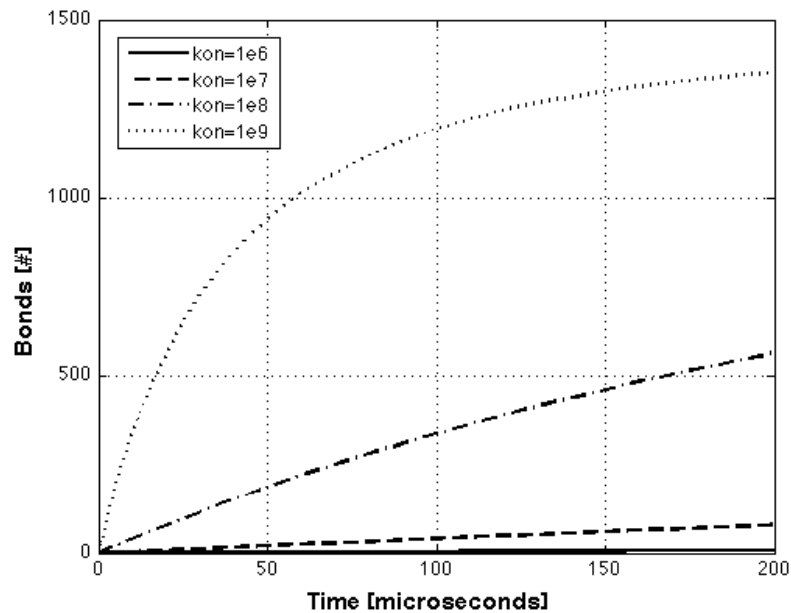


Figure 26: The number of bonds formed as a function of time at a shear rate of $10,000 \text{ s}^{-1}$, a platelet contact percentage of 10% and a receptor density of $500 \text{ domains}/\mu\text{m}^2$.

From Figure 25 we can see that as on-rate increases, bonds are formed more quickly. As the number of available receptors and ligands are consumed, the rate of bond formation decreases. At a platelet contact percentage of 10%, there are 2261 GPIIb/IIIa ligands and 1413 vWF-A1 receptors involved in the reaction. This means the maximum number of

bonds that can form is 1416. We expect that the number of bonds formed will asymptotically approach 1416 bonds. We can see that over the time period plotted, an on-rate of $10^9 \text{ M}^{-1}\text{s}^{-1}$ approaches this value. The model has predicted the binding reaction, as we would expect.

If we examine number of bonds versus time plots for other scenarios we can see what trends appear. Increasing shear rate does not affect the binding rate; it simply determines how quickly the binding reaction must occur. In the simulation shear rate is used to determine the time scales of the plots and the differential equation solver. If we increase the platelet contact percentage, the binding rate should increase as more receptors and ligands are available for binding.

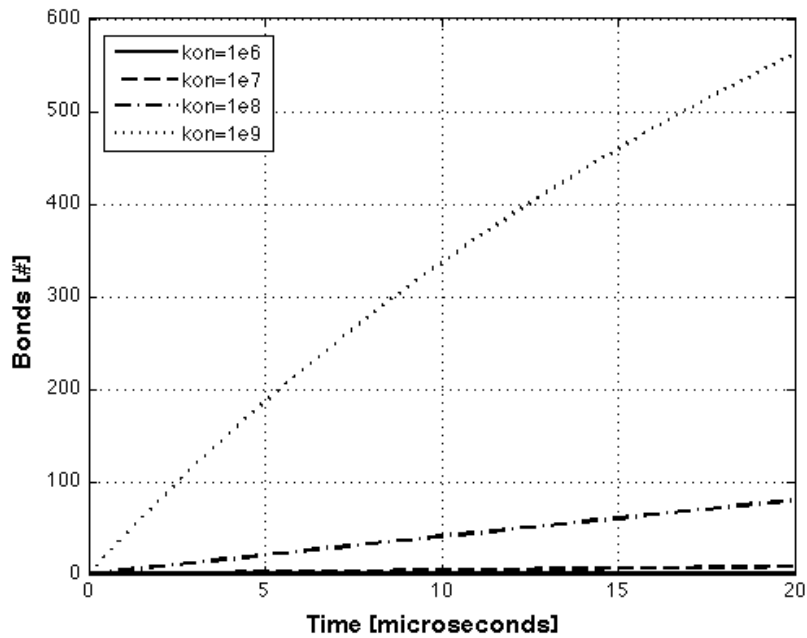


Figure 27: Number of bonds formed versus time at $100,000 \text{ s}^{-1}$, 10% platelet contact and $500 \text{ domains}/\mu\text{m}^2$.

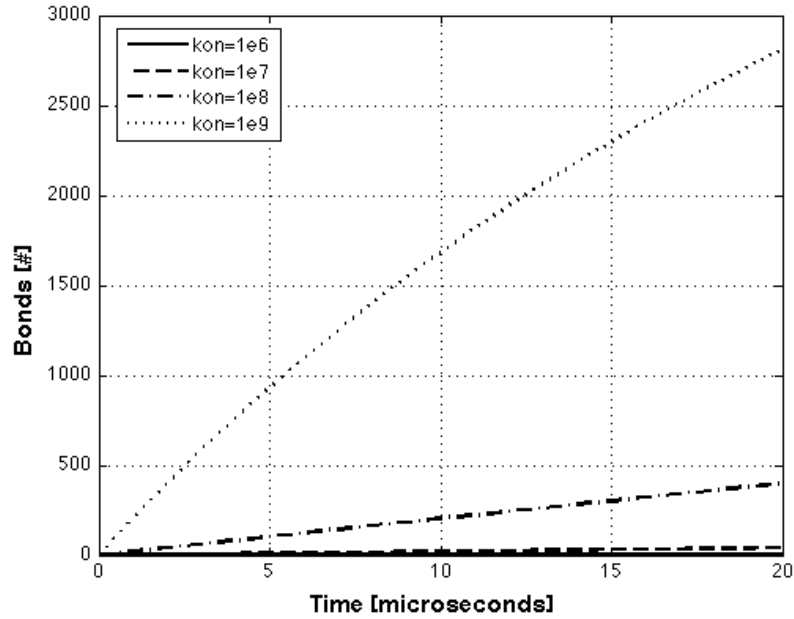


Figure 28: Number of bonds formed versus time at $100,000 \text{ s}^{-1}$, 50% platelet contact and $500 \text{ domains}/\mu\text{m}^2$.

By increasing the platelet contact percentage by 5, we see create a 5-fold difference in the maximum number of bonds formed.

We can also affect the binding rate by altering the domain density. By choosing the domain density created by globular vWF ($10 \text{ domains}/\mu\text{m}^2$) at a shear rate of $100,000 \text{ s}^{-1}$, we see the results demonstrated in Figure 28. In order to isolate the effects of changing the domain density we will leave the platelet contact percentage at 10%, even though globular vWF can only achieve 0.7% contact.

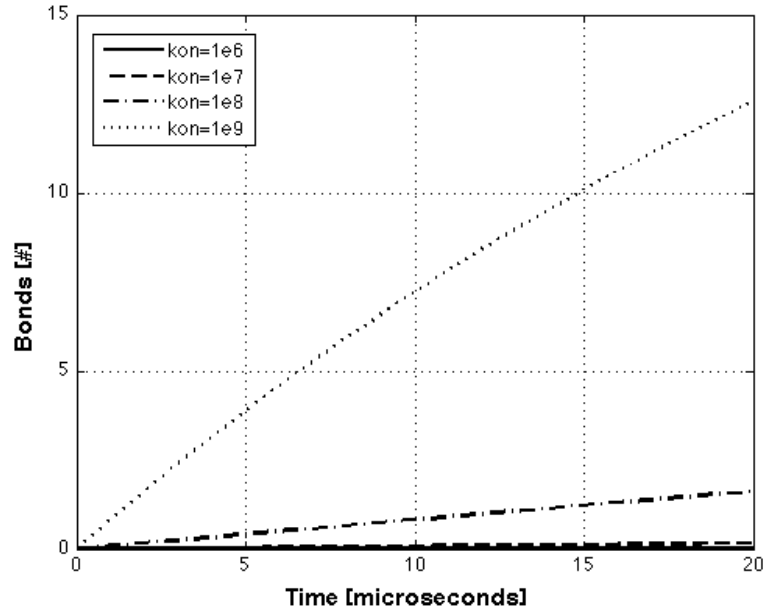


Figure 29: Number of bonds versus time at $100,000 \text{ s}^{-1}$, 10% platelet contact and 10 domains/ μm^2 .

If we increase the domain density by a factor of 100 we see the results in Figure 29.

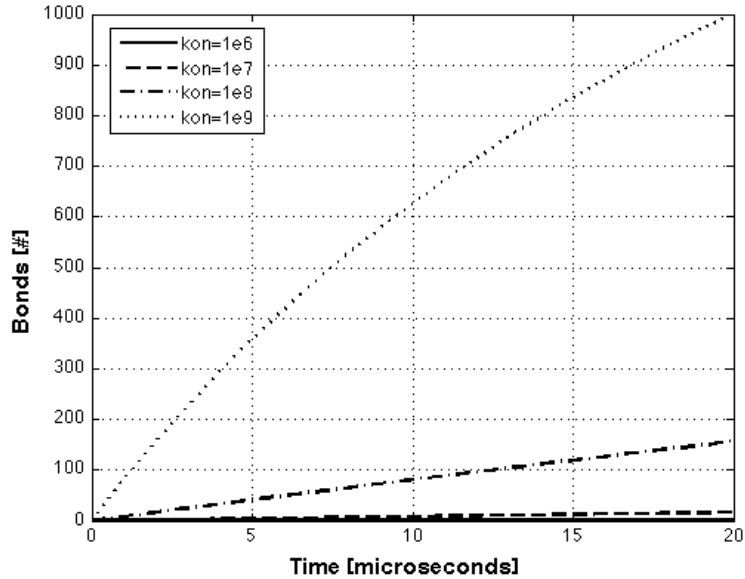


Figure 30: Number of bonds versus time at $100,000 \text{ s}^{-1}$, 10% platelet contact and 1000 domains/ μm^2 .

As with platelet contact percentage an increase in domain density sees an increase in binding rate. This would suggest that the increase in platelet contact percentage and domain density created by the unfolding of vWF should create a large increase in binding rate.

By demonstrating the linear relationships in the results between platelet contact percentage, domain density and on-rate, we have verified the behavior of the model according to the relationships outlined in Equation 12. The results from this aspect of the simulation are collected by the software loop described in Figure 24 and presented.

Binding Time versus Domain Density

For a given shear rate and platelet contact percentage, it is useful to demonstrate the relationship between domain density and binding time. Increasing domain densities

can represent the change from globular to elongated vWF as well as increases in local vWF concentration. The information from these plots can be used to determine what domain density, and what mechanisms, are necessary to capture a platelet at a given shear rate and platelet contact percentage.

By selecting the minimum time to form the required number of bonds from bonds-versus-time data at a particular shear rate, on-rate and platelet contact percentage, we can determine what domain density is required to capture a platelet in a certain amount of time. This process is illustrated in Figure 30.

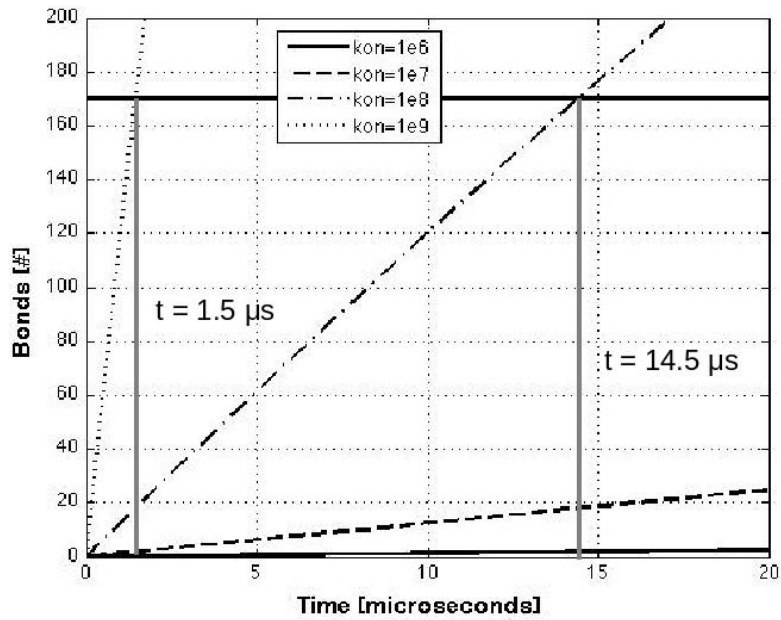


Figure 31: Illustration of time points used to create binding time versus domain density plots. Time points are from a simulation run at $100,000 \text{ s}^{-1}$, 10% platelet contact and $1500 \text{ domains}/\mu\text{m}^2$.

In Figure 30, the required number of bonds at this shear rate ($100,000 \text{ s}^{-1}$) 170; thus, on-rates of 10^9 and 10^8 can create 170 bonds in 1.5 and 14.5 microseconds, respectively, under these conditions. Therefore, at $1500 \text{ domains}/\mu\text{m}^2$ and $10^8 \text{ M}^{-1}\text{s}^{-1}$, the appropriate number of bonds is formed in 14.5 microseconds. This data point is added to a matrix that, when completed, is plotted. The process described in Figure 24 handles this process automatically. The final plots for selected scenarios are presented below.

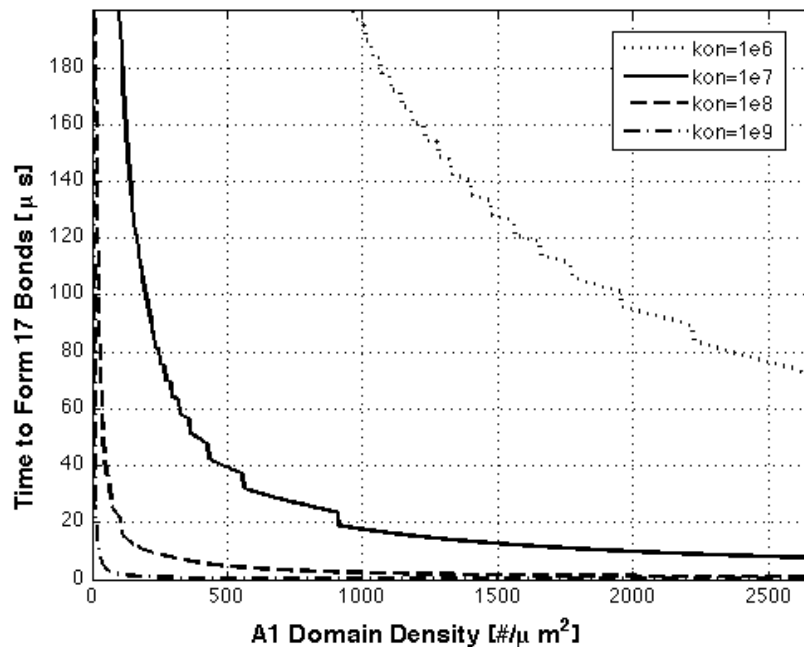


Figure 32: The time required to form the required number of bonds (17) versus the receptor density at a shear rate of $10,000 \text{ s}^{-1}$ and a platelet contact percentage of 10%.

As we can see from Figure 31, the exponential decay seen in the bonds versus time plots is reflected in time versus domain density. Decreases in domain density exponentially increase the amount of time it takes to form the necessary number of bonds. In this case all four of the selected on-rates are sufficient to form the necessary number of bonds in

required 150 microseconds and capture the platelet. The slower on-rates require greater densities of receptors to increase the reaction rate.

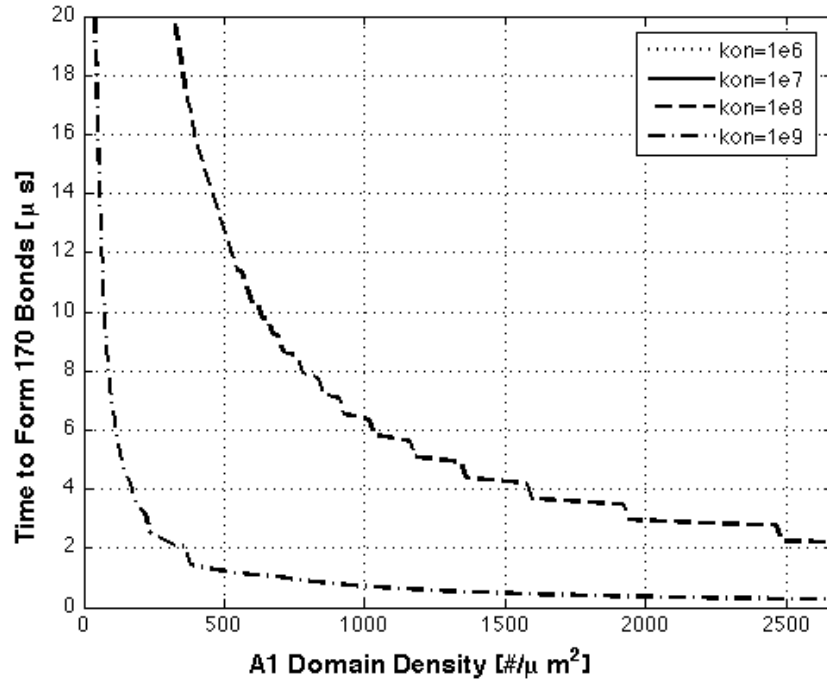


Figure 33: Binding time versus domain density at $100,000 \text{ s}^{-1}$ and 33% platelet contact.

As the shear rate increases, the range of sufficient on-rates decreases. At $100,000 \text{ s}^{-1}$ 10^6 and $10^7 \text{ M}^{-1}\text{s}^{-1}$ are not sufficient to capture a platelet even though the contact percentage increased.

From these binding time versus domain density plots we can determine the minimum density required to capture a platelet and make conclusions regarding elongation, activation, shear rate and on-rate. We select the minimum domain density from each binding time versus domain density plot (plots for all scenarios can be found in Appendix B) as is illustrated in Figure 33.

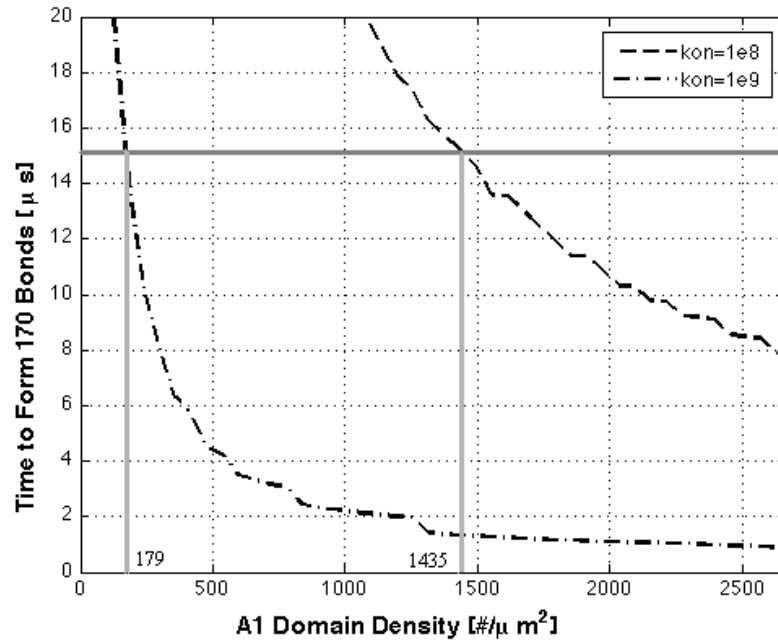


Figure 34: Binding time versus domain density at a shear rate of $100,000 \text{ s}^{-1}$ and a contact percentage of 10%. The horizontal line delineates the 15 microsecond binding time required to capture a platelet. The vertical lines represent the domain densities required to achieve capture by that time point.

Receptor Density vs. Shear Rate vs. On-rate vs. Contact Percentage

By compiling these receptor densities for each combination of shear rate, on-rate and platelet contact percentage we can create the following plots, which allow us to examine the effects of each variable.

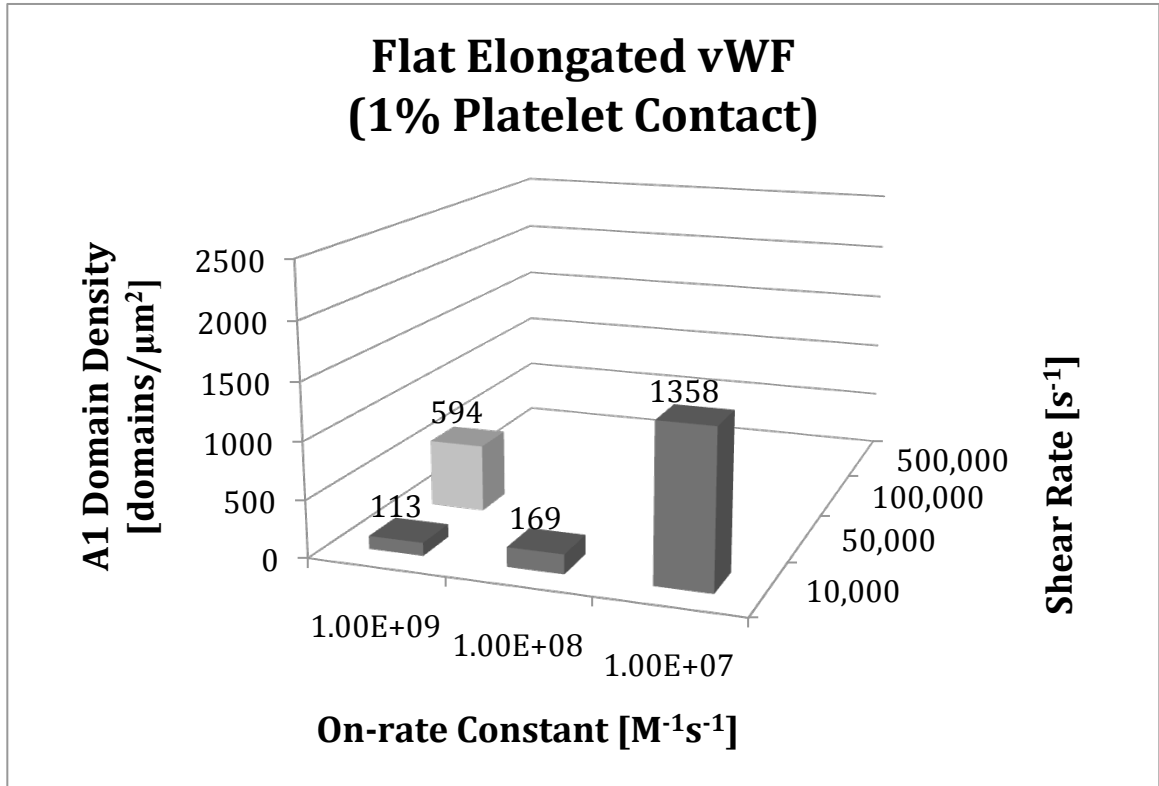


Figure 35: Required domain densities for platelet capture for flat elongated vWF with 1% platelet contact.

Flat elongated vWF is insufficient to capture platelets at $100,000 s^{-1}$ and requires a very fast on-rate at $50,000 s^{-1}$. An on-rate of $10^6 M^{-1}s^{-1}$ is insufficient to capture a platelet at $10,000 s^{-1}$ with 1% platelet contact. An on-rate of $10^7 M^{-1}s^{-1}$ requires a very high concentration of vWF to bind to the thrombus surface and align appropriately. As activation is required for domain densities greater than $50 \text{ domains}/\mu m^2$, activation is required to capture a platelet with flat, elongated vWF.

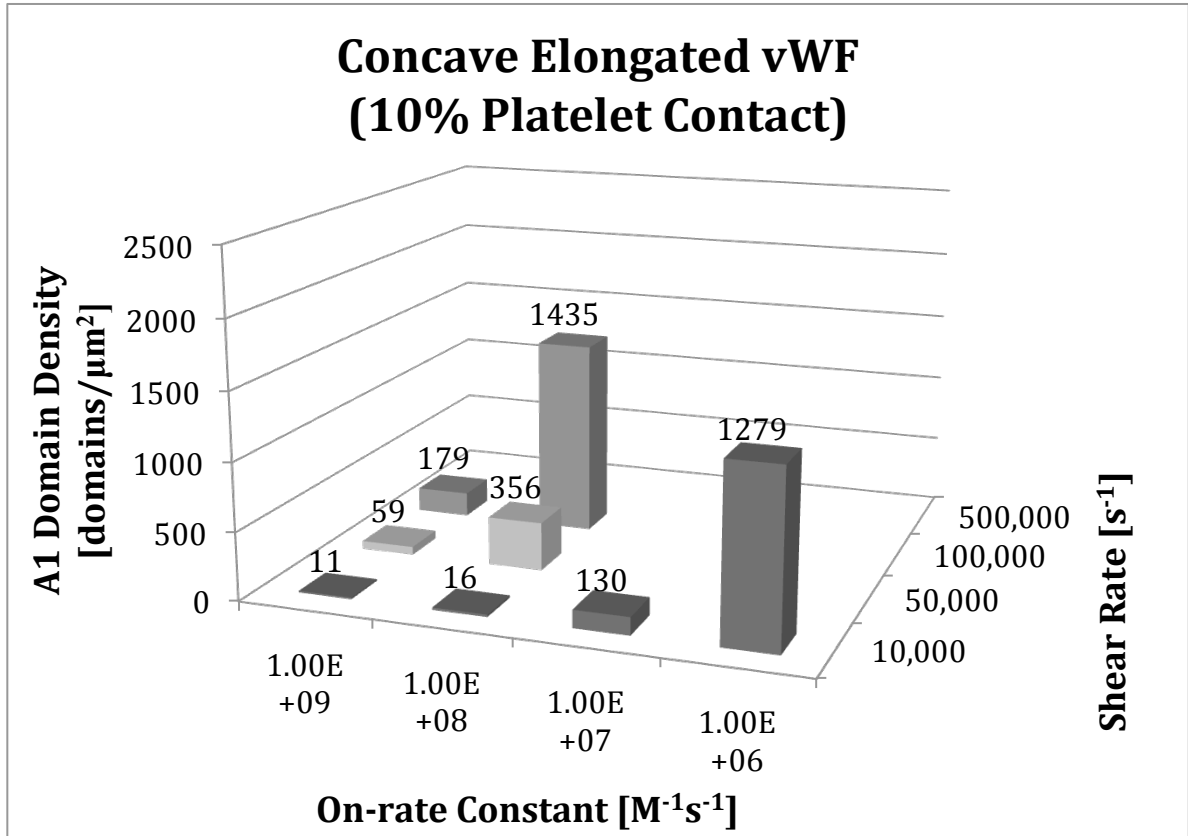


Figure 36: Required domain densities for platelet capture at 10% platelet contact.

At 10% platelet contact we see that platelet capture is not possible at $500,000 s^{-1}$ and requires a very fast on-rate at $100,000 s^{-1}$. We see that each of the four selected on-rates is sufficient for platelet capture at some domain density. An on-rate of $10^6 M^{-1}s^{-1}$ requires a very high domain density to capture a platelet with 10% platelet contact. At 10% platelet contact, activation is required at $50,000 s^{-1}$ and greater.

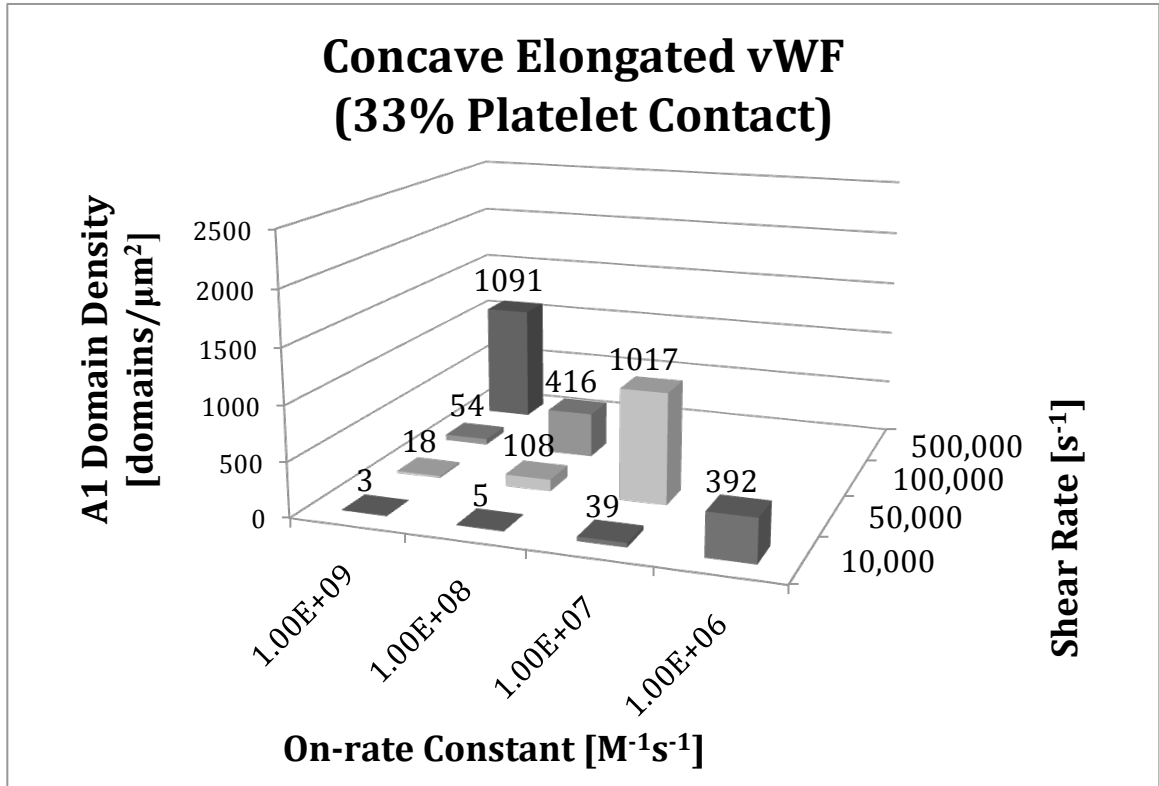


Figure 37: Required domain densities for platelet capture at 33% platelet contact.

A platelet contact percentage of 33% is sufficient to capture a platelet at 500,000 s⁻¹ with a very fast on-rate and a very high domain density. Activation is required for capture at 500,000 s⁻¹. All four selected on-rates are sufficient for platelet capture at 33% platelet contact.

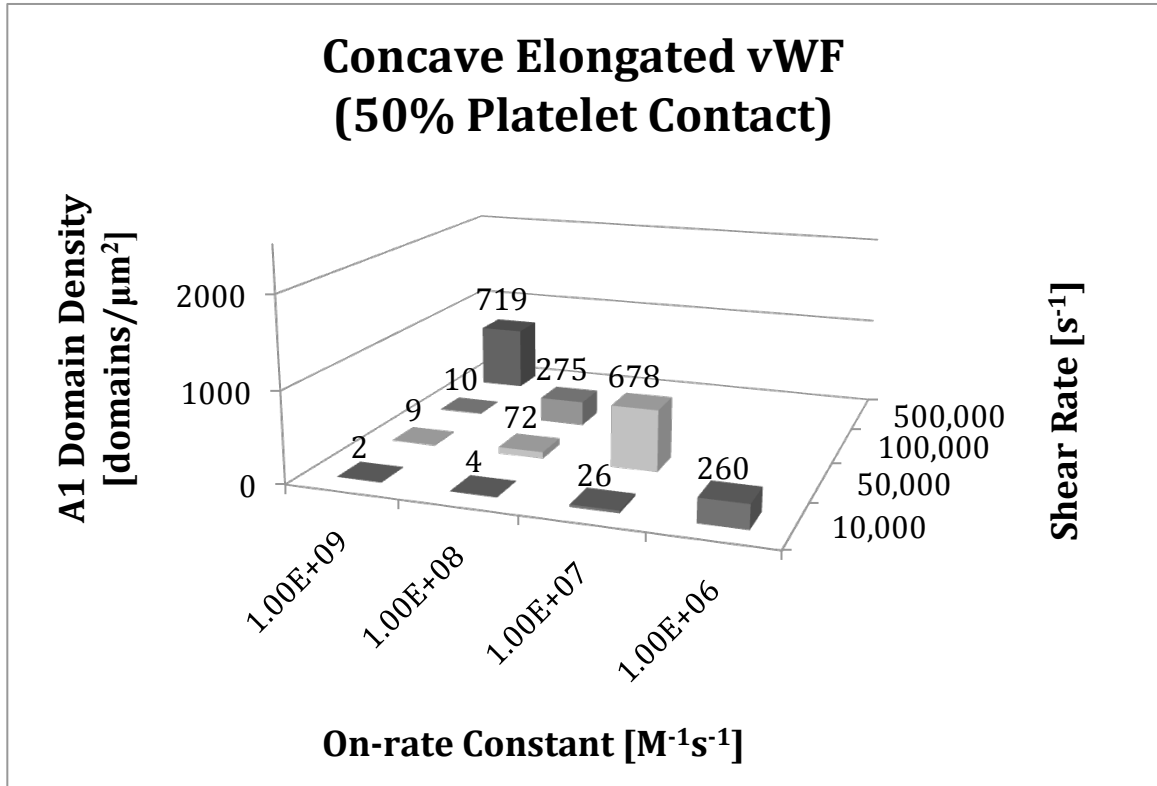


Figure 38: Required domain densities for platelet capture at 50% platelet contact.

A platelet contact percentage of 50% is sufficient for platelet capture at with a fast on rate constant and a high domain density. Activation is required for platelet capture at $500,000\ s^{-1}$ at 50% platelet contact. All four on-rate constants are sufficient for platelet capture at 50% contact.

Globular vWF showed no data over this range of on-rates and shear rates; thus, platelet capture is not possible with globular vWF at the shear rates we have considered. With a maximum contact percentage of 0.07% and a maximum domain density of 10 domains/ μm^2 , globular vWF has a maximum of 1 A1 receptor available for binding. This means that globular vWF can form, at most, one bond with a platelet. Consequently, the maximum shear rate at which globular vWF is sufficient for platelet capture is $1,000\ s^{-1}$.

At this shear rate and domain density, an on-rate constant of $10^8 \text{ M}^{-1}\text{s}^{-1}$ is required to capture the platelet. At a shear rate of $\sim 1,000 \text{ s}^{-1}$, globular vWF begins to unfold [Schneider et al, 2007]. This suggests that vWF unfolding occurs at the shear rate at which unfolded vWF becomes necessary.

DISCUSSION

Thrombotic platelet accumulation is a critical mechanism in hemostasis that can also cause pathologic arterial occlusions [Ku, 1997]. For arterial stenoses, the local peak shear can reach $600,000 \text{ s}^{-1}$ [Bark and Ku, 2010]. Thus, platelet capture and adhesion can occur at very high shear rates. Our results use experimental data on GPIIb/IIIa-vWF-A1 bonding to describe one way of achieving platelet capture at these high shear rates through simultaneous activation release of vWF, elongation of the vWF molecule, and the formation of concave surfaces to match the high density of GPIIb/IIIa already present on circulating platelets. This study suggests a mechanism for high shear platelet capture that demonstrates the possible importance of vWF elongation and platelet activation to capture a platelet in high shear. The vWF molecule shape change allows for very high densities of receptors to be exposed on the thrombus surface. Platelet activation allows a high density of these molecules to assemble on the thrombus surface. We have demonstrated the conditions that allow platelet capture under our model in terms of the amount and contour of vWF, the on-rate constant, and the shear rate.

Summary of Results

There are five major conclusions from this study. First, our model suggests that multiple bonds are necessary to capture a platelet above $\sim 600 \text{ s}^{-1}$. Multiple bonds have been suggested by previous work as a possible mechanism for overcoming large unbinding forces. Multiple simultaneous bonds have also been demonstrated in AFM experiments [Sulchek et al, 2005]. However, the simultaneous bonding of hundreds of bonds may be a unique mechanism to capture millions of circulating platelets under the

very high shear rates and drag forces for hemostasis. We have analyzed the binding of a platelet to a surface of vWF, but we have not addressed how this surface adheres to the aggregate. By the same force balance used in this study, the vWF must adhere to the aggregate with the appropriate number of bonds. The number of bonds necessary to adhere the vWF surface and platelet to the aggregate is determined by the force of each bond and the drag force created by the platelet and vWF surface in flow.

The second result of the model is that vWF unfolding is necessary for the exposure of multiple A1 domains within the footprint of a platelet. A globular vWF would not be expected to have many A1 domains on its exterior surface, whereas an elongated strand of vWF could expose many more A1 domains. Unfolding of vWF has been demonstrated at shears above $5,000 \text{ s}^{-1}$ and would be consistent with the hypothesis that the increased domain densities created by elongated vWF could aid in platelet capture [Ruggeri, 2001, Ruggeri et al, 2006, Schneider et al, 2007].

A third consequence of the modeling indicates that overlapping strands of vWF can work in combination to provide more binding sites to capture a platelet at a shear rate of $50,000 \text{ s}^{-1}$ with on-rates less than $10^8 \text{ M}^{-1}\text{s}^{-1}$. At higher shear rates, hundreds of bonds are required, necessitating multiple strands of vWF within a small volume. In order to create the large density of bond receptors, a high concentration of vWF should remain near the surface of the aggregate. These multiple strands would likely come from the local release of vWF from platelets on the thrombus surface that have been activated by lengthened exposure to very high shear stress. The multiple strands could entangle to form a net of strands with a very high density of A1 domains. Images of vWF under

shear suggest the surface of the thrombus could be coated with a net-like array of elongated vWF molecules [Schneider et al, 2007].

Fourth, a concave contour with greater than 1% surface contact is necessary for platelet capture above $50,000 \text{ s}^{-1}$ for on-rates less than $10^9 \text{ M}^{-1}\text{s}^{-1}$. Greater platelet contact allows many ligands and receptors to increase the binding rate between the platelet and the surface. The concave contour could form pockets where platelets could create up to a thousand bonds between GPIIb/IIIa and A1 receptors. As the three-dimensional vWF surface is not uniform, one would expect thrombus to form in patches and not in uniform layers, which has been observed in experiments of platelet aggregation at high shears [Ku and Flannery, 2007]. Thus, the increasing number of surface A1 receptors as shear increased would match the existing high density of platelet GPIIb/IIIa ligands, leading to a Velcro-like immediate adhesion from hundreds of similarly spaced bonds. However, since concave contours are spaced and often filled, one would expect that the probability of capture would decrease as shear rates become pathologically high.

A fifth result establishes that the on-rate for GPIIb/IIIa binding to vWF-A1 may be greater than $10^8 \text{ M}^{-1}\text{s}^{-1}$ under hemodynamic shear conditions above $10,000 \text{ s}^{-1}$. Miura et al report an on-rate of $\sim 1,000 \text{ M}^{-1}\text{s}^{-1}$ with bonding times of $\sim 100 \text{ sec}$ [Miura et al, 2000]. Doggett indicate a bond time a thousand fold faster at $\sim 0.1 \text{ s}$ [Doggett et al, 2003]. Mody et al calculate an on-rate of $\sim 6 \times 10^5 \text{ M}^{-1}\text{s}^{-1}$ [Miura et al, 2000, Mody and King, 2008]. These values can differ by a factor of 600, probably due to 4 order of magnitude errors that can come from surface plasmon resonance measurements. The on-rate constants required in our model are two orders of magnitude faster than other

intercellular bonds previously reported. This could be due to the necessity for quick binding in hemostasis.

vWF Unfolding

We have demonstrated that vWF elongation is necessary for high shear platelet capture by our model. By elongating vWF, vWF-A1 densities can increase by greater than 17 times and allow platelets to adhere with multiple bonds. The elongated vWF strands can cross link to form a net with 20 times the available A1 domains in a square micron. The ability for vWF to create a variety of contours allows it to contact more of the platelet surface, accessing more GPIIb/IIIa ligands. A concave pocket on the surface of the thrombus allows up to 37 times more A1 domains for binding with platelet GPIIb/IIIa.

Conversely, globular vWF in plasma concentrations should not be able to capture a circulating platelet above $1,000 \text{ s}^{-1}$ if only GPIIb/IIIa-vWF-A1 binding is used. Thus, other bonds such as GPIIb/IIIa and fibrinogen may be more functional at the lower shear rates.

Our study mechanically describes how vWF unfolding can affect the platelet binding process. The use of quantitative modeling demonstrates the synergistic relationship between the vWFA1 domain density, the vWF contour and the on-rate to achieve platelet capture at shear rates up to $500,000 \text{ s}^{-1}$. The amounts of ligands and receptors necessary to capture a platelet in our model could provide a reason for the exceedingly high amounts of GPIIb/IIIa ligands on the platelet surface.

Activated-Platelet Release of vWF

In order to achieve the high domain densities provided by multiple strands of elongated vWF, platelet-activated release of vWF is necessary. vWF concentrations released from platelets upon activation are 50 times higher than vWF concentrations in the plasma. vWF released from platelets is also released locally. This local release can allow a larger percentage of the vWF to come in contact with the thrombus surface. Previous studies have suggested local high concentrations of vWF may be essential for high shear platelet capture [Ruggeri and Mendolicchio, 2007].

Limitations

There are some critical limitations and assumptions in this study. First, Equation 8 is based on equilibrium binding. Equilibrium binding may not be an accurate description of the platelet-wall interaction. Unfortunately, a more accurate description of non-equilibrium cell-surface binding is beyond the scope of this paper [Hammer and Lauffenberger, 1987]. A model that better describes a cell with membrane-bound ligands attaching to a surface of receptors would be a valuable future development for the understanding of this, and other, cell binding reactions. Second, we have assumed that there exists no undiscovered 20,000 pN bond that could adhere a platelet to a thrombus without multivalency. Third, we have assumed that on-rates, off-rates, and fluid velocities remain constant. On-rates and off-rates can change with applied forces [Yago et al, 2007, Kumar et al, 2003]. This would allow for low on-rates at low shear that can increase with shear to accommodate for decreased binding time. However, bonds with these characteristics, like catch bonds, typically release at very high shear forces.

Previous models have considered dissociation rates that change with force, based on the Bell model [Mody and King, 2008]. We have instead assumed an overall bond strength of 100 pN for simplicity. While it is also likely that fluid velocities, and thus shear forces, will change with pulsatile flow or thrombus growth, we have considered steady flow for this analysis. Lastly, we have assumed that the vWF surface responsible for capturing the platelet is stably bound to the aggregate. To determine if the vWF surface can withstand the drag forces of the platelet(s) bound to it, a force balance must be performed between the bonds that bind the surface to the aggregate and the drag forces on the platelet(s) and vWF.

A phenomenon often seen in platelet adhesion is rolling. As platelets collide with the binding surface they form transient bonds that form and break causing the platelet to roll along the surface. Our model does not consider rolling, but our model can be iteratively applied to each collision and describe the discrete events of the rolling process. As a platelet forms a bond with the surface and breaks free its velocity is slowed. Now, with a lower velocity the platelet has a greater binding time and can form more bonds. This process can continue until the platelet is traveling slow enough to form the appropriate platelet bond strength with the surface. Iteratively applying our model with new, slower, input velocities will simulate each individual binding attempt in a discrete fashion. However, *in vitro* experiments have shown that platelets can accumulate at the *upstream* end of the stenosis. This implies that there has been little if any rolling before capture. Thrombosis that occurs on implanted mechanical devices such as artificial valves and stents would also require capture over very short distances and short time-scales. Platelets are able to adhere to edges of devices despite the short surface lengths

that cannot accommodate rolling across the surface. A study by Ruggeri et al in 2006 demonstrates that as shear rates increase and vWF plays a more predominant role, platelet adhesion switches from rolling to adherent attachment [Ruggeri, 2006]. The implications of platelet rolling do not effect the conclusions of this study. Our model concentrates on the final interaction of the rolling process where the platelet creates a permanent attachment to the surface irrespective of prior rolling.

Future Work

A number of conclusions from this study can and should be verified experimentally. Additionally, the conclusions of this study point to new areas of experimentation that can further elucidate the ideas set forth in this study.

First, to determine the true range of achievable vWF-A1 densities, labeled vWF can be flowed over a surface and imaged. By labeling the A1 domains on vWF with gold nanoparticles and releasing high concentrations into a blood flow over a layer of mural thrombus, the vWF can unfold and expose its domains. Gluteraldehyde can then be used to fix the vWF in its elongated formation for imaging using SEM.

Second, multiple bonds between a platelet and a thrombogenic surface can be demonstrated by laying down vWF, in a similar fashion as described above, and dragging a platelet fixed to an AFM tip over it. As the platelet binds and unbinds, the force versus time data can demonstrate the number of unbinding events. This is similar to a study by Sulchek et al in 2005 [Sulchek et al, 2005].

Third, platelets can be flowed over surfaces with known receptor densities to determine if capture is possible. This would serve to validate Figures 34-37 while also narrowing the range of possible on-rate constants.

Lastly, images of vWF conformations relative to bound platelets from an actual thrombus could verify and give further insight into the role of vWF contour in platelet capture.

Implications of Results

As hemostasis is life preserving, the need for platelet aggregation at very high shear rates is critical. The progressive release, unfolding, and network conformation of vWF allows increasing platelet binding to vWFA1 under elevated shear without inducing the capture of platelets at low shear. As life-preserving high shear platelet aggregation becomes less relevant in modern day life, high shear thrombosis may become a health risk. Turning off this mechanism by inhibiting one of the steps described in this study, such as vWF unfolding, could allow for low shear hemostasis without the health risks of high shear arterial thrombosis.

Knowledge and future evidence of the mechanism described in this paper could lead to drug developments that may help reduce the pathologic consequences of high shear thrombosis. Preventing vWF release from platelets or depleting their vWF supply may reduce local vWF concentrations and hinder high shear binding. As a newer avenue of attack, interference with vWF unfolding may eliminate high shear adhesion altogether. Bleeding times from platelet adhesion with globular vWF would not be affected, but the high shear adhesion involved in arterial thrombosis could be prevented.

CONCLUSIONS

This study demonstrates that activation coupled with vWF elongation can explain the very high shear platelet capture that occurs in severe stenoses. Elongation and activation combine to form contoured surfaces coated in a high density of vWF-A1 domains that capture platelets with large contact areas, high receptor-ligand concentrations and a fast on-rate constant. Manipulation of this mechanism could lead to highly specific antithrombotic drugs for the prevention of occlusive arterial thrombosis.

APPENDIX A

MATLAB Simulation Code

```
clear all
clc

%inputs (time in microseconds)
shearrate=1000; %force on cell in piconewtons (must be a 1 and zeros)
bondstrength=100; %strength of bond in piconewtons
vel=shearrate*1.5e-6; %cell velocity in m/s
bindspot=3e-6; %distance cell must travel to be out of binding area in m
lpsm=800; %ligands per square micron on cell surface
rpsm=10; %receptors per square micron on binding surface
rpsmmax=2664; %maximum per square micron density of receptors
C=0.007; %platelet surface area contacting the surface [percent]
sep=45; %length of ligand molecule [nm]
kon1=1e6; %a possible binding association rate [M^-1*s^-1]
kon2=1e7; %a possible binding association rate [M^-1*s^-1]
kon3=1e8; %a possible binding association rate [M^-1*s^-1]
kon4=1e9; %a possible binding association rate [M^-1*s^-1]
koff=5; %the dissociation rate [s^-1]

%obtain bonds, assoctime, binding vol, receipts and lignds
force=6*pi*4e-3*1.5e-6*1.5e-6*shearrate*1e12;
sa=C*4*pi*(1.5)^2;
b=floor(force/bondstrength);
assoctime=bindspot/vel;
V=sa*10^(-12)*sep*10^(-9)*1000;
r=rpsm*sa;
l=lpsm*sa;
rmax=rpsmmax*sa;

rwork=b:b:rmax;
rr=rwork./sa;

Cl=l/V
Cr=r/V

%buffer assoctime (for density plot)
excess=.5e-6;
trim=.1e-6;
atrun=assoctime+excess;
atrimd=atrun-trim;
span1=.1;
span2=.05;
span3=.005;
span4=.0005;

%establish empty matrices (for density code)
tt1=zeros(max(rwork)/b,1);
tt2=zeros(max(rwork)/b,1);
tt3=zeros(max(rwork)/b,1);
tt4=zeros(max(rwork)/b,1);
```

```

%find number of bonds formed as a function of time
for n=1:1:4;
    kon=eval(['kon' num2str(n)]);
    [t Y]=ode45(@hpsabvt,[0 asstocme],[0],[],r,l,V,kon,koff);
    eval(['t_' num2str(n) '=t']);
    eval(['y_' num2str(n) '=Y']);
end

%find 10 bond time points of simulations at 4 onrates and different
%densities (for density plots)
for n=b:b:rmax;
    rs=n;
    c=(n./b);
    [t,y]=ode45(@hpsatvd,[0 atrun],[0 0 0 0],[],rs,l,V,kon1,kon2,kon3,kon4,koff);
    [h1,i1]=min(abs(y(:,1)-b));
    [h1,i2]=min(abs(y(:,2)-b));
    [h1,i3]=min(abs(y(:,3)-b));
    [h1,i4]=min(abs(y(:,4)-b));
    tt1(c,1)=t(i1);
    tt2(c,1)=t(i2);
    tt3(c,1)=t(i3);
    tt4(c,1)=t(i4);
end

%trim arrays (for density plots)
[h2,i5]=min(abs(tt1-atrimd));
[h2,i6]=min(abs(tt2-atrimd));
[h2,i7]=min(abs(tt3-atrimd));
[h2,i8]=min(abs(tt4-atrimd));

t1=tt1(i5:1:max(rwork)/b).*10^6;
t2=tt2(i6:1:max(rwork)/b).*10^6;
t3=tt3(i7:1:max(rwork)/b).*10^6;
t4=tt4(i8:1:max(rwork)/b).*10^6;

r1=rr(i5:1:max(rwork)/b);
r2=rr(i6:1:max(rwork)/b);
r3=rr(i7:1:max(rwork)/b);
r4=rr(i8:1:max(rwork)/b);

%smooth data (for density plots)
%t1smooth=mallowess(r1,t1,'Span',span1);
%t2smooth=mallowess(r2,t2,'Span',span2);
%t3smooth=mallowess(r3,t3,'Span',span3);
%t4smooth=mallowess(r4,t4,'Span',span4);

%extra outputs
Nav=6.022e23;
BRon1=kon1.*(1-10).*(((r-10)./V)./Nav)
BRon2=kon2.*(1-10).*(((r-10)./V)./Nav)
BRon3=kon3.*(1-10).*(((r-10)./V)./Nav)
BRon4=kon4.*(1-10).*(((r-10)./V)./Nav)
BROff=koff*10

%plotting
figure(1)

```

```

plot(t_1*10^6,y_1,'-k','LineWidth',2)
hold on
plot(t_2*10^6,y_2,'--k','LineWidth',2)
hold on
plot(t_3*10^6,y_3,'-.k','LineWidth',2)
hold on
plot(t_4*10^6,y_4,':k','LineWidth',2);ylabel('Bonds [#] ', 'fontsize',12,'fontweight','b'), xlabel('Time
[microseconds] ', 'fontsize',12,'fontweight','b')
h=legend('kon=1e6','kon=1e7','kon=1e8','kon=1e9',4);
set(h,'Interpreter','none')
axis([0 500 0 10])
grid on

figure(2)
plot(r1,t1,':k','LineWidth',2);ylabel('Time to Form 170 Bonds [ \mus] ', 'fontsize',12,'fontweight','b'),
xlabel('A1 Domain Density [#/\mum^{2}] ', 'fontsize',12,'fontweight','b')
hold on
plot(r2,t2,'-k','LineWidth',2)
hold on
plot(r3,t3,'--k','LineWidth',2)
hold on
plot(r4,t4,'-.k','LineWidth',2)
hold on
%semilogx(r1,t1smooth,':k','LineWidth',2)
%hold on
%semilogx(r2,t2smooth,'-k','LineWidth',2)
%hold on
%semilogx(r3,t3smooth,'--k','LineWidth',2)
%hold on
%semilogx(r4,t4smooth,'-.k','LineWidth',2);ylabel('Time to Form 170 Bond [ \mus]
','fontsize',12,'fontweight','b'), xlabel('A1 Domain Density [#/\mum^{2}] ', 'fontsize',12,'fontweight','b')
h=legend('kon=1e6','kon=1e7','kon=1e8','kon=1e9',4);
set(h,'Interpreter','none')
axis([0 rpsmmax 0 (assotime*10^6)])
grid on

```

APPENDIX B

Binding Time vs. Domain Density Plots

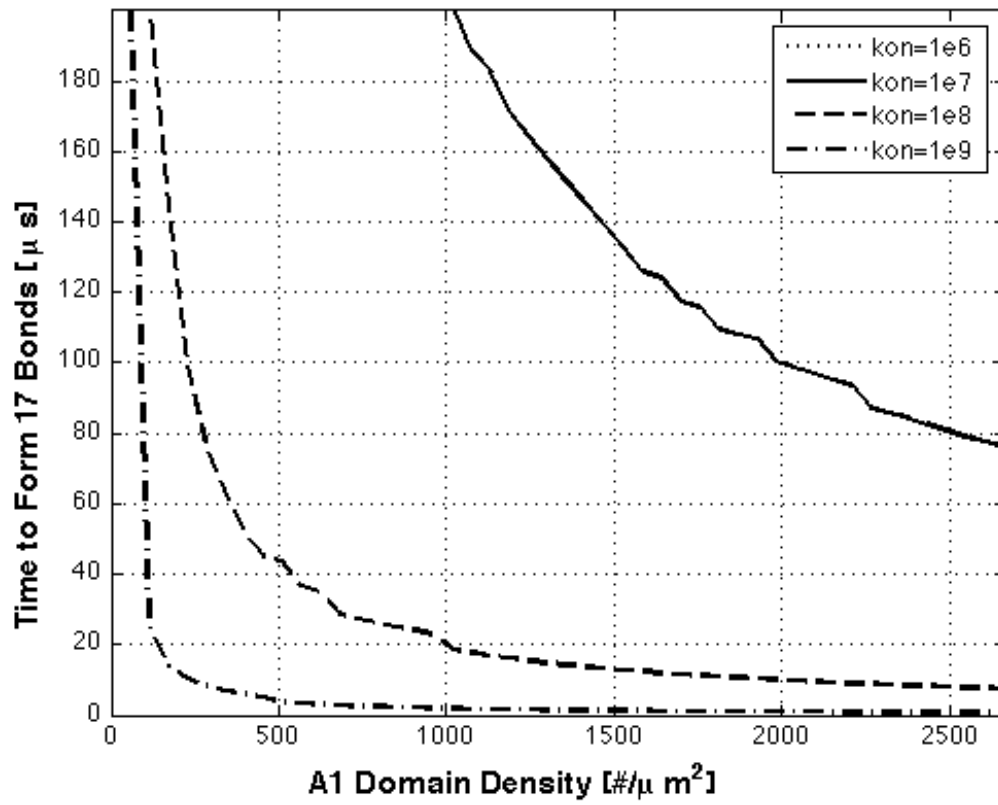


Figure 39: Binding time versus domain density at $10,000 \text{ s}^{-1}$ and 1% platelet contact.

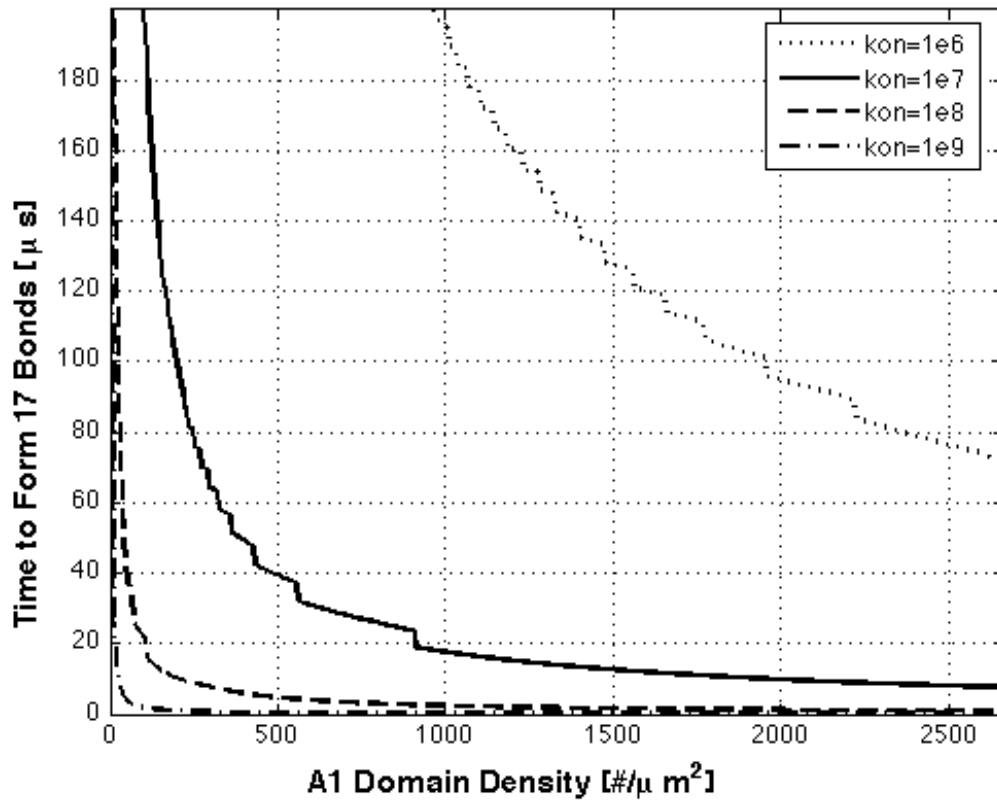


Figure 40: Binding time versus domain density at $10,000 \text{ s}^{-1}$ and 10% platelet contact.

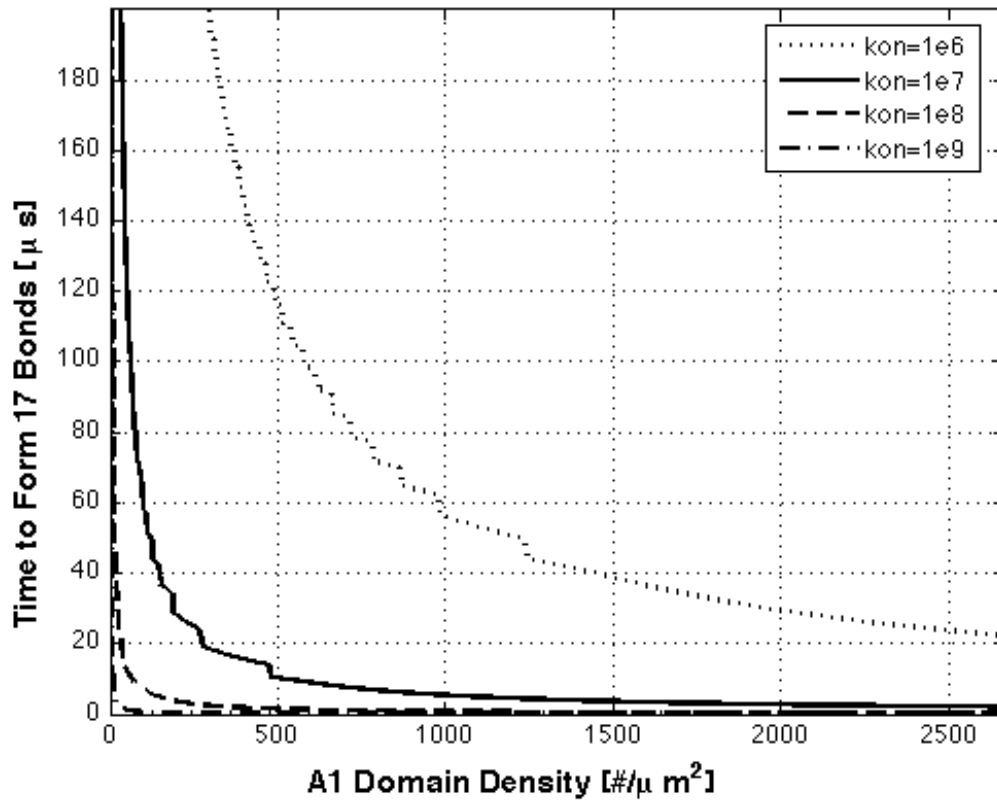


Figure 41: Binding time versus domain density at $10,000 \text{ s}^{-1}$ and 33% platelet contact.

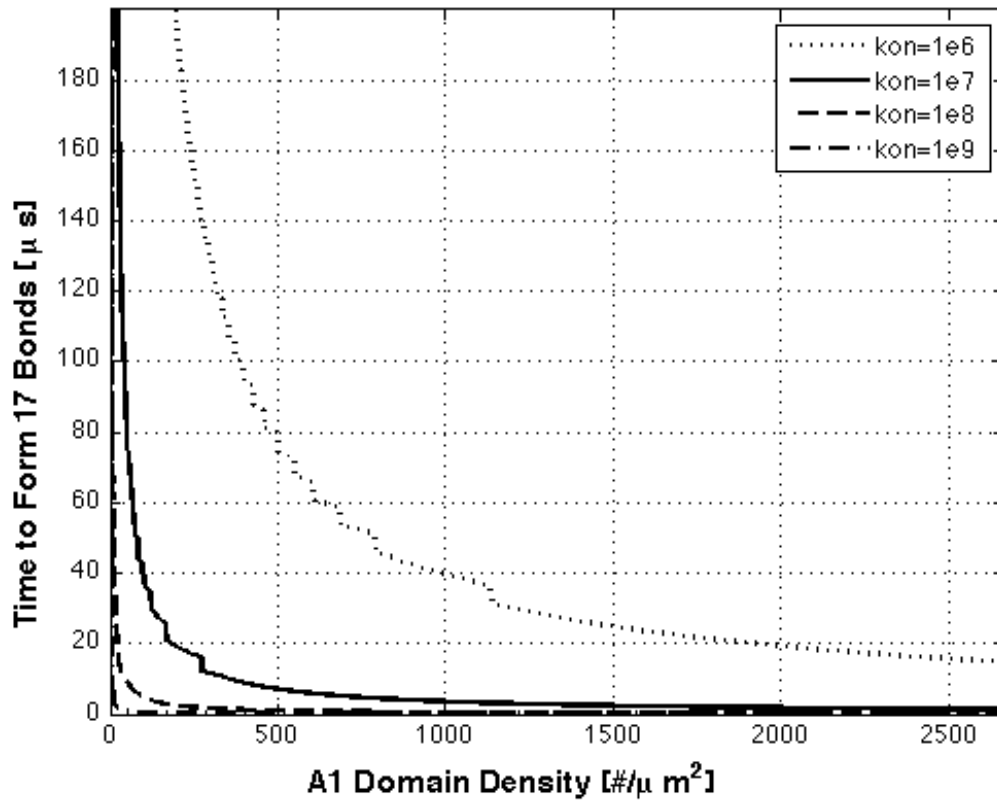


Figure 42: Binding time versus domain density at $10,000 \text{ s}^{-1}$ and 50% platelet contact.

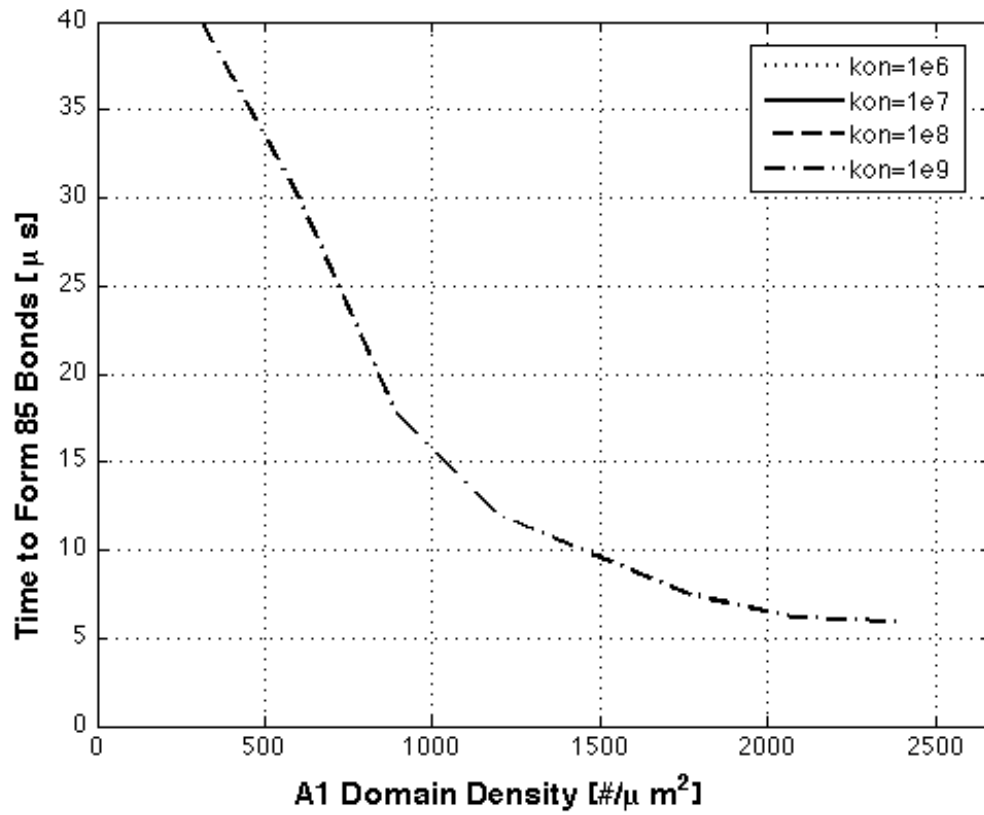


Figure 43: Binding time versus domain density at $50,000 \text{ s}^{-1}$ and 1% platelet contact.

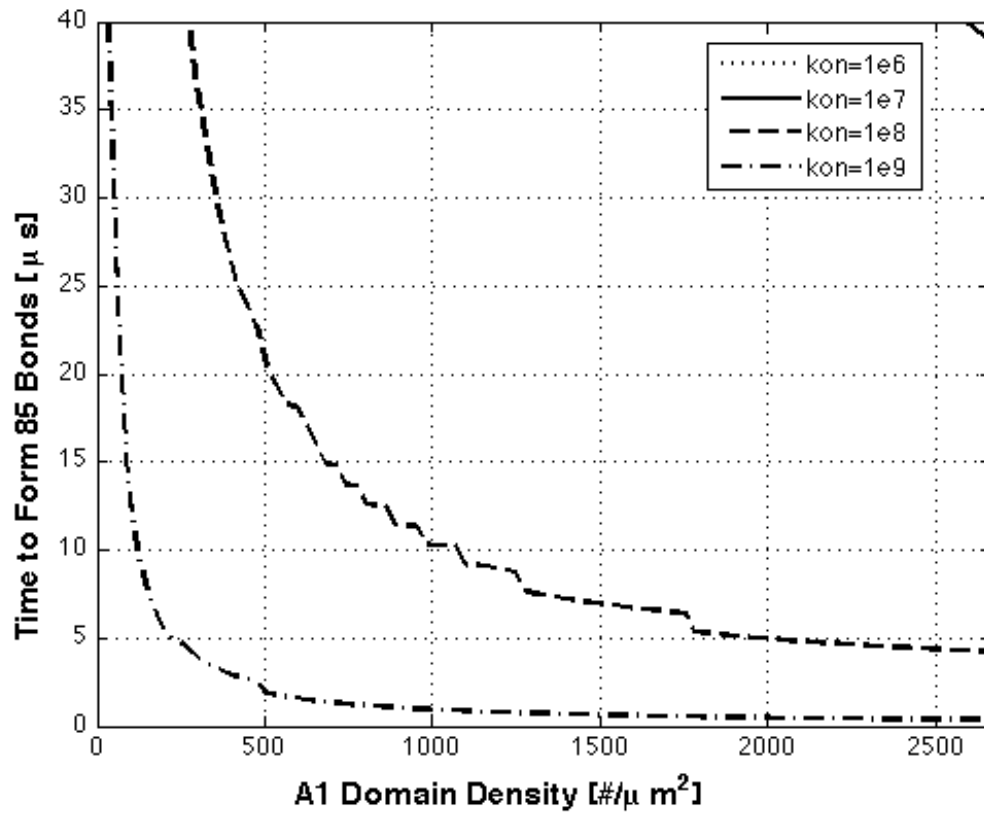


Figure 44: Binding time versus domain density at $50,000 \text{ s}^{-1}$ and 10% platelet contact.

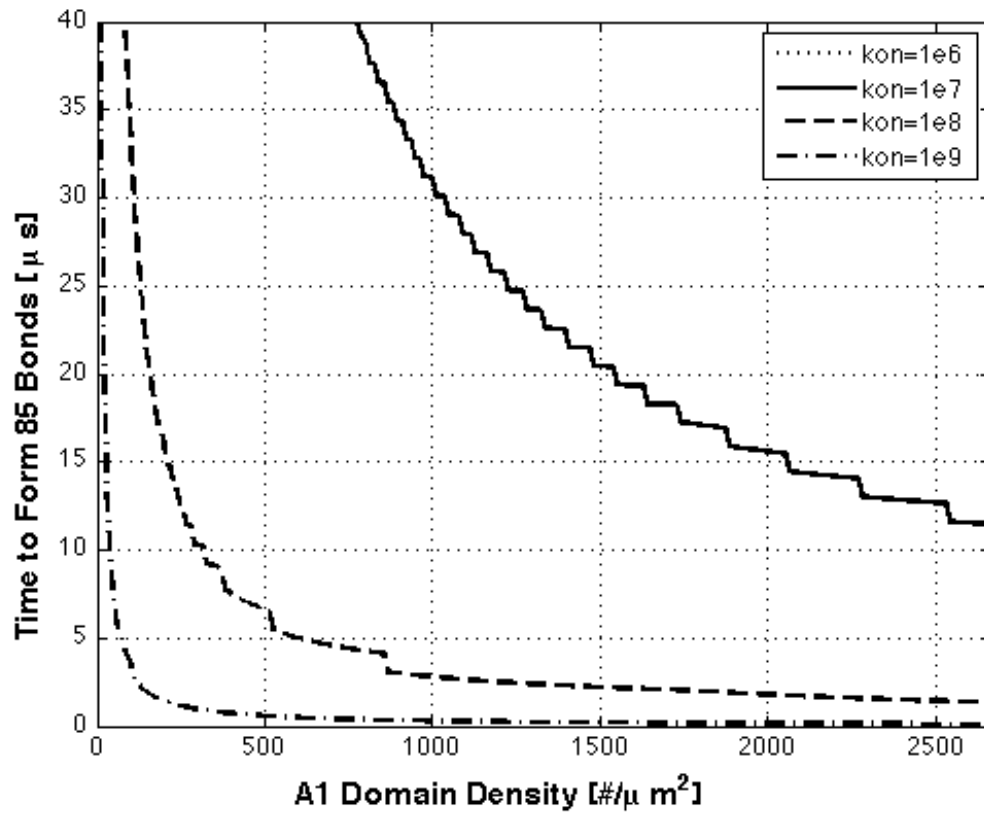


Figure 45: Binding time versus domain density at 50,000 s⁻¹ and 33% platelet contact.

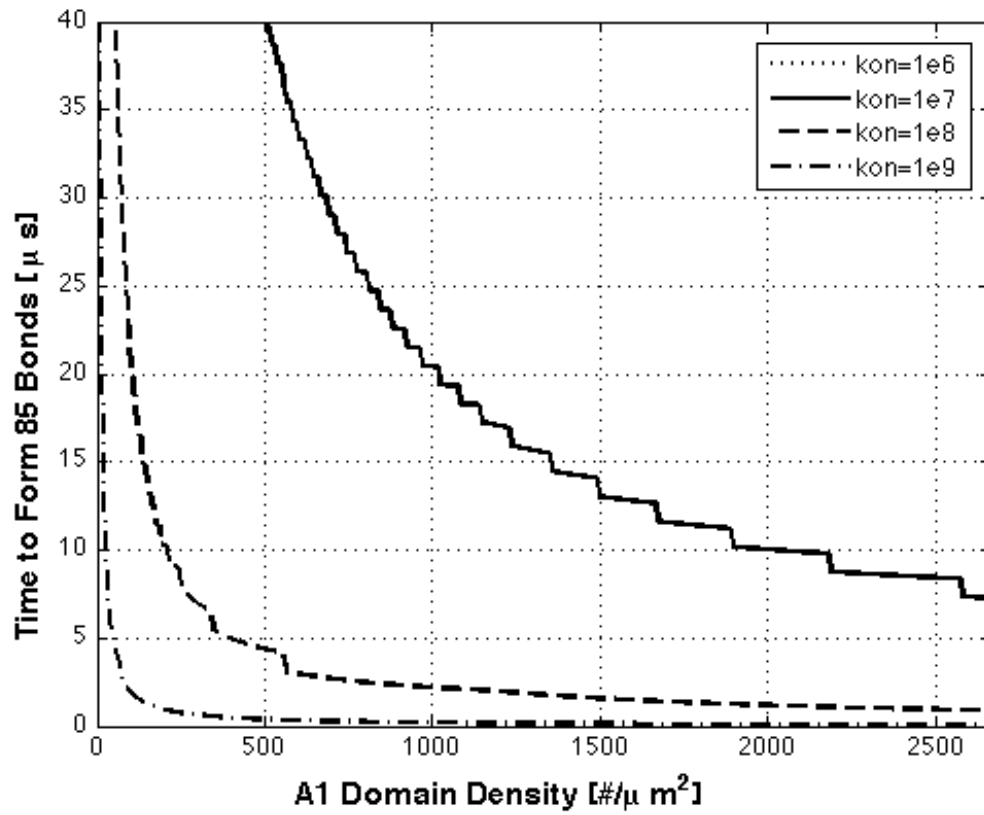


Figure 46: Binding time versus domain density at $50,000 \text{ s}^{-1}$ and 50% platelet contact.

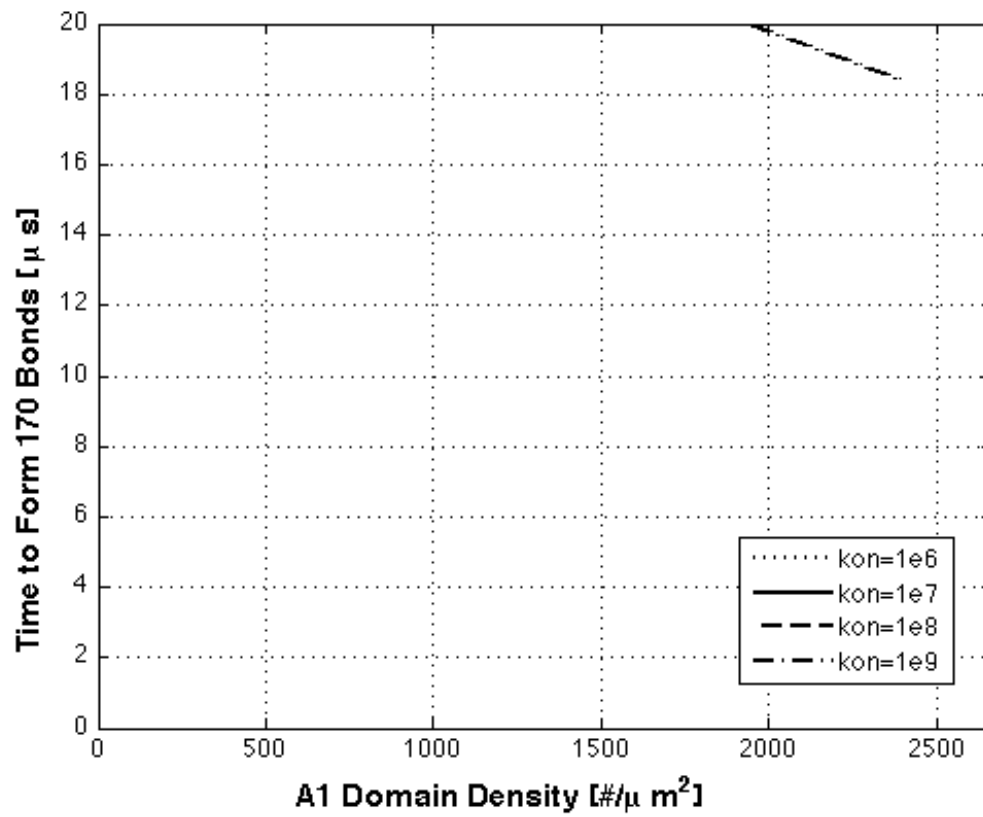


Figure 47: Binding time versus domain density at $100,000 \text{ s}^{-1}$ and 1% platelet contact.

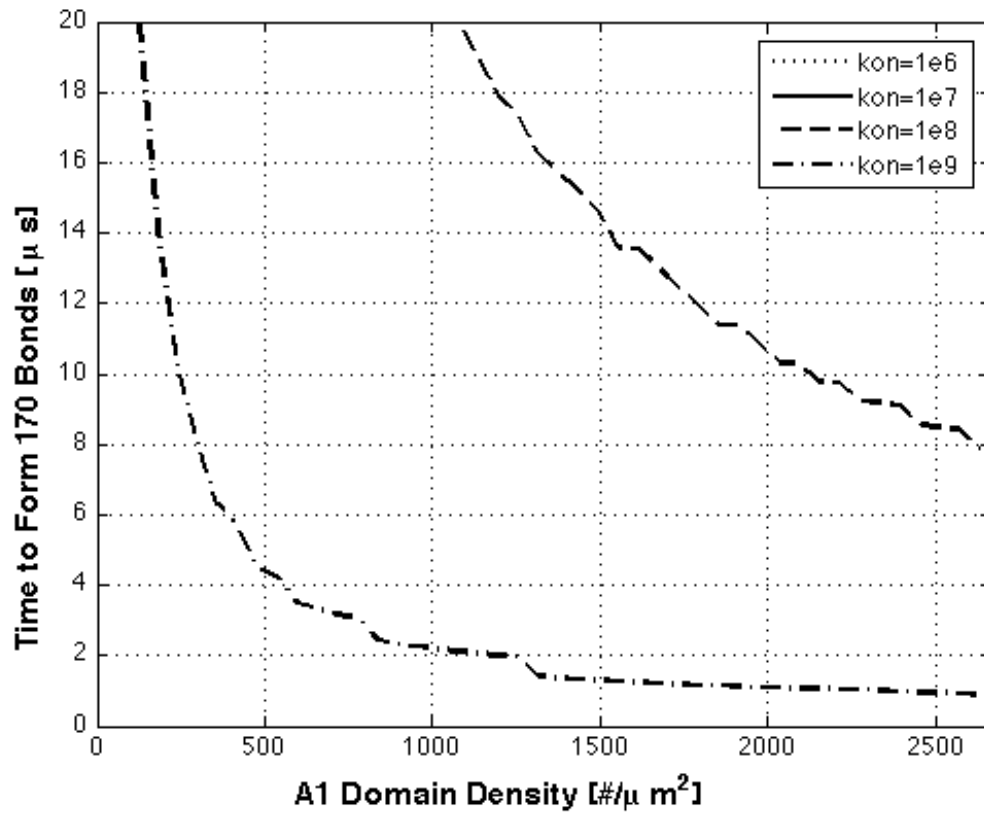


Figure 48: Binding time versus domain density at $100,000 \text{ s}^{-1}$ and 10% platelet contact.

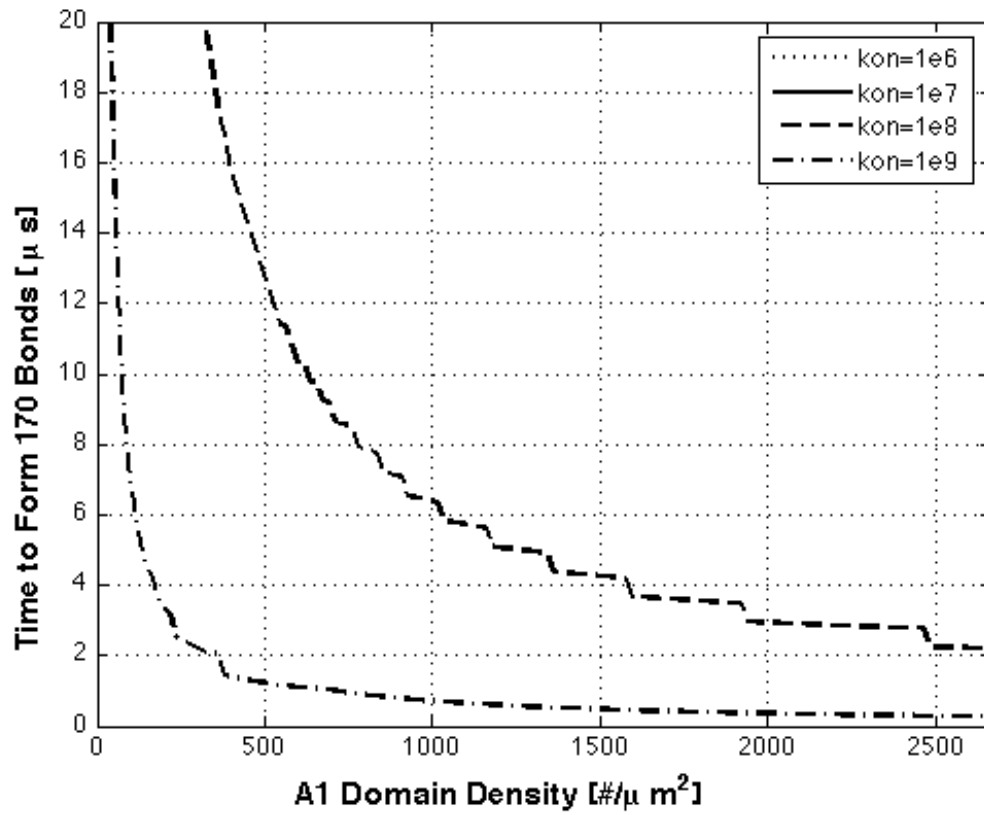


Figure 49: Binding time versus domain density at $100,000 \text{ s}^{-1}$ and 33% platelet contact.

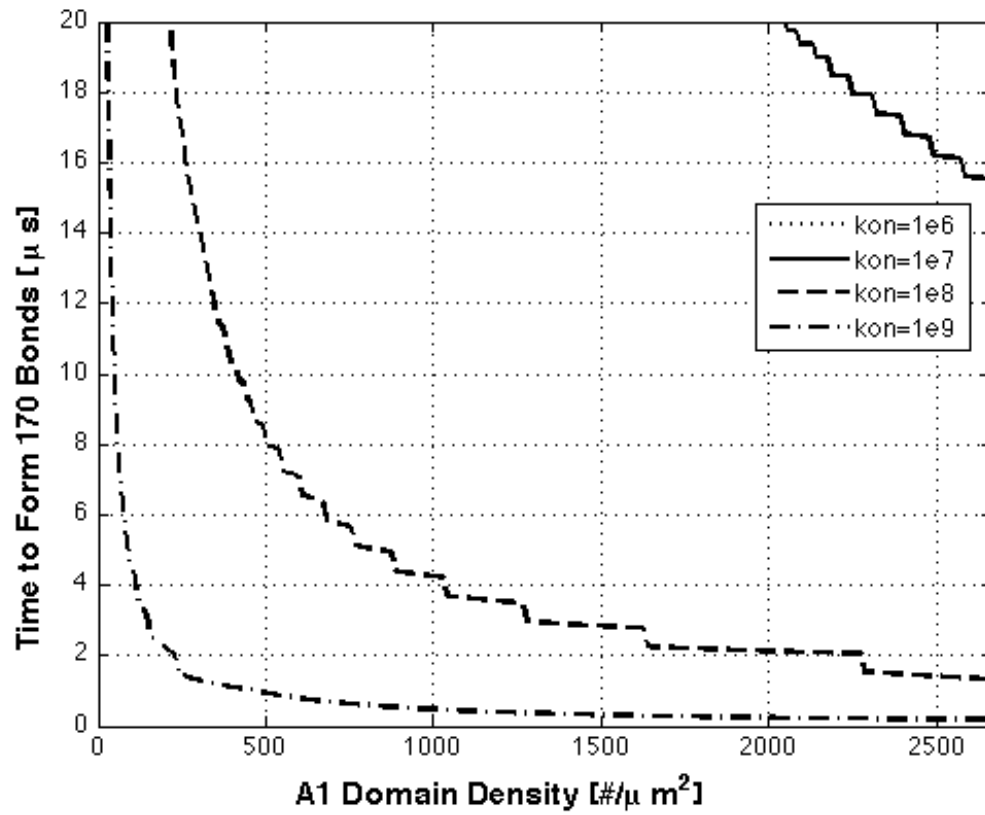


Figure 50: Binding time versus domain density at $100,000 \text{ s}^{-1}$ and 50% platelet contact.

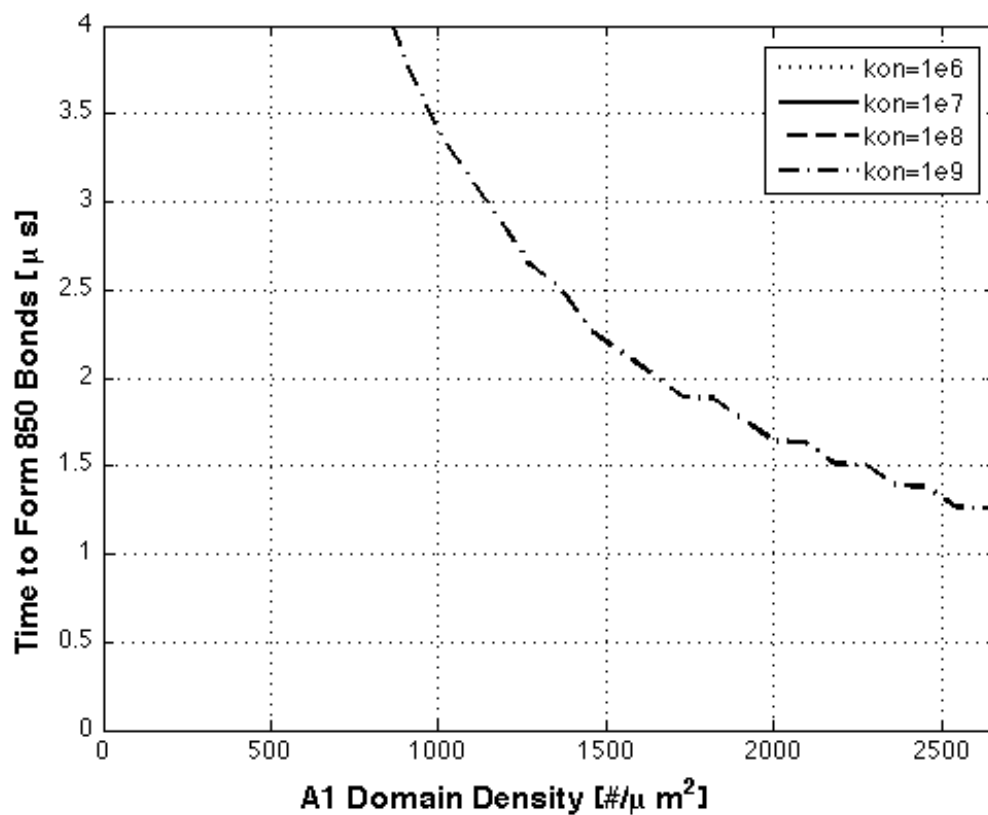


Figure 51: Binding time versus domain density at $500,000 \text{ s}^{-1}$ and 33% platelet contact.

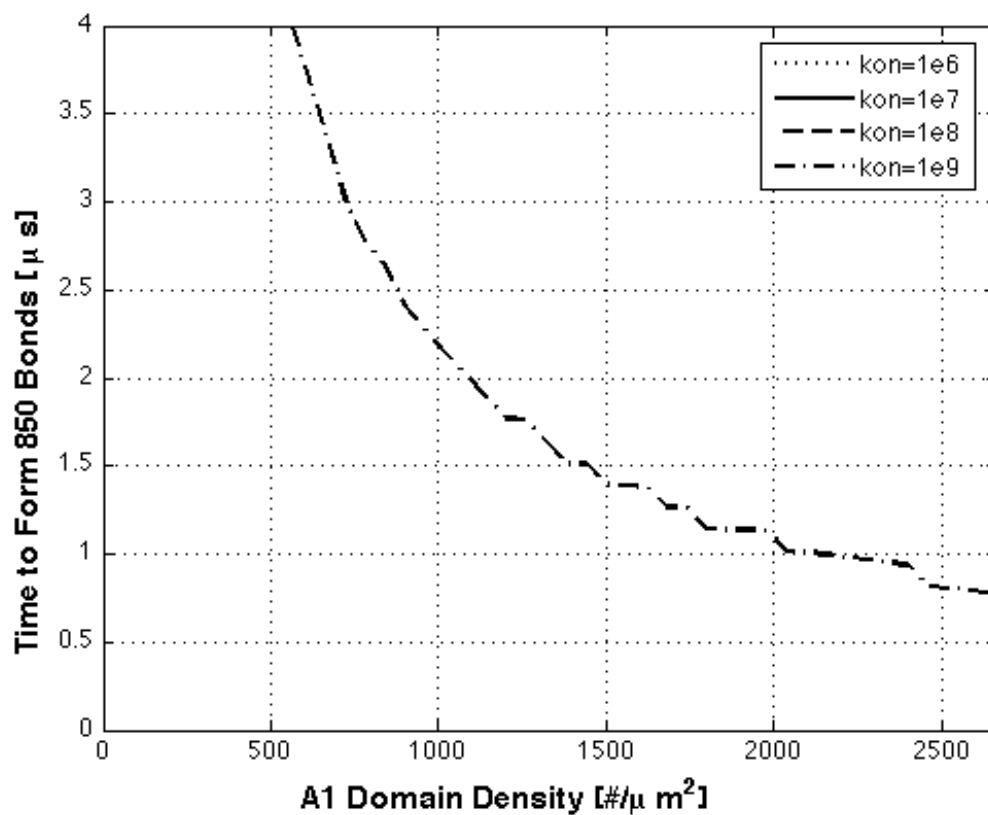


Figure 52: Binding time versus domain density at $500,000 \text{ s}^{-1}$ and 50% platelet contact.

REFERENCES

- Arya, M., A. B. Kolomeisky, G. M. Romo, M. A. Cruz, J. A. Lopez and B. Anvari. 2005. Dynamic force spectroscopy of glycoprotein Ib-IX and von Willebrand factor. *Biophys. J.* 88:4391-4401.
- Bark, D. L. and D. N. Ku. 2010. Wall shear over high degree stenoses pertinent to atherothrombosis. *J. Biomech.* USA. 43:2970-2977.
- Bell, G. I. 1978. Models for the specific adhesion of cells to cells. *Science.* USA. 200:618-627.
- Berndt, M. C., C. Gregory, A. Kabral, H. Zola, D. Fournier and P. A. Castaldi. 1985. Purification and preliminary characterization of the glycoprotein Ib complex in the human platelet membrane. *Euro. J. Biochem.* UK. 151:637-649.
- Davies, M. J. and A. Thomas. 1984. Thrombosis and acute coronary-artery lesions in sudden cardiac ischemic death. *N. Engl. J. Med.* USA. 310:1137-40.
- Doggett, T. A., G. Girdhar, A. Lawshe, D. W. Schmidtke, I. J. Laurenzi, S. L. Diamond and T. G. Diacovo. 2002. Selectin-like kinetics and biomechanics promote rapid platelet adhesion in flow: the GPIb α -vWF tether bond. *Biophys. J.* USA. 83:194-205.
- Doggett, T. A., G. Girdhar, A. Lawshe, J. L. Miller, I. J. Laurenzi, S. L. Diamond and T. G. Diacovo. 2003. Alterations in the intrinsic properties of the GPIb α -VWF tether bond define the kinetics of the platelet-type von Willebrand disease mutation, Gly233Val. *Blood.* USA. 102:152-160.
- Dong, J. F., C. Q. Li, G. S. Tung, W. Hyun, V. A. Kharghan and J. A. Lopez. 1997. The cytoplasmic domain of glycoprotein (GP) Ib α constrains the lateral diffusion of the GP Ib-IX complex and modulates von Willebrand factor binding. *Biochemistry.* USA. 36:12421-12427.
- Fowler, W. E., L. J. Fretto, K. K. Hamilton, H. P. Erickson and P. A. McKee. 1985. Substructure of human von Willebrand factor. *J. Clin. Invest.* USA. 76:1491-1500.
- Galdi, G. P., R. Rannacher, A. M. Robertson and S. Turek. 2008. *Hemodynamical flows: modeling, analysis and simulation.* Birkhauser Verlag Basel, Switzerland.
- Goldman A. J., R. G. Cox and H. Brenner. 1967. Slow viscous motion of a sphere parallel to a plane wall – II Couette flow. *Chem. Eng. Sci.* USA. 22:653–660.
- Hammer, D. A. and D. A. Lauffenburger. 1987. A dynamical model for receptor-mediated cell adhesion to surfaces. *Biophys. J.* USA. 52:475-487.

- Harrison, P., and E. M. Cramer. 1993. Platelet α -granules. *Blood Reviews*. USA. 7:52-62.
- King, M. R., and D. A. Hammer. 2001. Multiparticle adhesive dynamics: hydrodynamic recruitment of rolling leukocytes. *Proc. Natl. Acad. Sci. USA*. 98:14919-14924.
- Krasik, E. F., K. L. Yee, and D. A. Hammer. 2006. Adhesive dynamics simulation of neutrophil arrest with deterministic activation. *Biophys. J.* USA. 91:1145-1155.
- Kroll, M. H., J. D. Hellums, L. V. McIntire, A. L. Schafer and J. L. Moake. 1996. Platelets and shear stress. *Blood*. USA. 88:1525-1541.
- Ku, D. N. 1997. Blood flow in arteries. *Annu. Rev. Fluid Mech.* USA. 29:399-434.
- Ku, D. N. and C. J. Flannery. 2007. Development of a flow-through system to create occluding thrombus. *Biorheology*. USA. 44:273-284.
- Kumar R. A., J. F. Dong, J. A. Thaggard, M. A. Cruz, J. A. Lopez and L. V. McIntire. 2003. Kinetics of GPIIb/IIIa-vWF-A1 tether bond under flow: effect of GPIIb/IIIa mutations on the association and dissociation rates. *Biophys. J.* USA. 85:4099-4109.
- Marston S. B. 1982. The rates of formation and dissociation of actin-myosin complexes. *Biochem. J.* UK. 203:453-460.
- Maxwell, M. J., S. M. Dopheide, S. J. Turner and S. P. Jackson. 2006. Shear induces a unique series of morphological changes in translocating platelets: effects of morphology on translocation dynamics. *Arterioscler. Thromb. Vasc. Biol.* USA. 26:663-669.
- Mehta, P., R. D. Cummings and R. P. McEver. 1998. Affinity and kinetic analysis of P-selectin binding to P-selectin glycoprotein ligand-1. *J. Biol. Chem.* USA. 273:32506-32513.
- Miura, S., C. Q. Lui, Z. Cao, H. Wang, M. R. Wardell and J. E. Sadler. 2000. Interaction of von Willebrand factor domain A1 with platelet glycoprotein IIb/IIIa-(1-289). *J. Biol. Chem.* USA. 275: 7539-7546.
- Mody N. A. and M. R. King. 2008. Platelet adhesive dynamics. Part II: high shear-induced transient aggregation via GPIIb/IIIa-vWF-GPIIb/IIIa bridging. *Biophys. J.* USA. 95:2556-2574.
- Nicholson, M. W., A. N. Barclay, M. S. Singer, S. D. Rosen and P. A. van der Merwe. 1998. Affinity and kinetic analysis of L-selectin (CD62L) binding to glycosylation-dependent cell-adhesion molecules. *J. Biol. Chem.* USA. 273:763-770.
- Paulus, J. M. 1975. Platelet size in man. *Blood*. USA. 46:321-336.

- Ruggeri, Z. M. 2001. Structure of von Willebrand factor and its function in platelet adhesion and thrombus formation. *Best Prac. Res. Clin. Haematol.* USA. 14:257-279.
- Ruggeri, Z. M., J. N. Orje, R. Habermann, A. B. Federici and A. J. Reininger. 2006. Activation-independent platelet adhesion and aggregation under elevated shear stress. *Blood.* USA. 108:1903-1910.
- Ruggeri, Z. M. and G. L. Mendolicchio. 2007. Adhesion mechanisms in platelet function. *Circ. Res.* USA. 100:1673-1685.
- Sadler, J. E. 1998. Biochemistry and genetics of von Willebrand factor. *Annu. Rev. Biochem.* USA. 67:395-424.
- Sadler, J. E. 2005. von Willebrand factor: two sides of a coin. *J. Thromb. Haemost.* 3:1702-1709.
- Salmon, E. D., M. McKeel and T. Hays. 1984. Rapid rate of tubulin dissociation from microtubules in the mitotic spindle in vivo measured by blocking polymerization with colchicine. *J. Cell. Biol.* USA. 99:1066-1075.
- Savage, B., J. J. Sixma and Z. M. Ruggeri. 2002. Functional self-association of von Willebrand factor during platelet adhesion under flow. *Proc. Natl. Acad. Sci.* USA. 99:425-430.
- Schlessinger, J., D. E. Koppel, D. Axelrod, K. Jacobson, W. W. Webb, and E. L. Elson. 1978. Lateral transport on cell membranes: mobility of concanavalin A receptors on myoblasts. *Cell Biol.* USA. 73:2409-2413.
- Schneider, S. W., S. Nuschele, A. Wixforth, C. Gorzelanny, A. Alexander-Katz, R. R. Netz and M. F. Schneider. 2007. Shear-induced unfolding triggers adhesion of von Willebrand factor fibers. *Proc. Natl. Acad. Sci.* USA. 104:7899-7903.
- Sulchek T. A., R. W. Friddle, K. Langry, E. Y. Lau, H. Albrecht, T. V. Ratto, S. J. DeNardo, M. E. Colvin and A. Noy. 2009. Dynamic force spectroscopy of parallel individual Mucin1-antibody bonds. *Proc. Natl. Acad. Sci.* USA. 102:16638-16643.
- Trusky G. A., F. Yuan and D. F. Katz. 2004. *Transport Phenomena in Biological Systems.* Pearson Education, Upper Saddle River, New Jersey, USA.
- Yago, T., V. I. Zarnitsyna, A. G. Klopocki, R. P. McEver and C. Zhu. 2007. Transport governs flow-enhanced cell tethering through L-selectin at threshold shear. *Biophys. J.* USA. 92:330-342.
- Yago, T., J. Lou, T. Wu, J. Yang, J. J. Miner, L. Coburn, J. A. Lopez, M. A. Cruz, J. Dong, L. V. McIntire, R. P. McEver and C. Zhu. 2008. Platelet glycoprotein Iba.

- forms catch bonds with human WT vWF but not with type 2B von Willebrand disease vWF. *J. Clin. Invest.* USA. 118:3195-3207.
- Zhang, Q., Y. Zhou, C. Zhang, X. Zhang, C. Lu and T. A. Springer. 2009. Structural specializations of A2, a force-sensing domain in the ultralarge vascular protein von Willebrand factor. *Proc. Natl. Acad. Sci.* USA. 106:9226-9231.
- Zhao, R., M. V. Kameneva and J. F. Antaki. 2007. Investigation of platelet margination phenomena at elevated shear stress. *Biorheology.* USA. 44:161-177.